

P 2mif



**COLOR ILLUSTRATIONS REPRODUCED
IN BLACK AND WHITE**

EVALUATION OF MULTIBAND PHOTOGRAPHY
FOR ROCK DISCRIMINATION

By

Gary L. Raines



Remote Sensing Report 74-2

NASA Grant NGL-06-001-015

USAROD Grant DA-ARO-D31-124-71-G101

USAROD Grant DA-ARO-D31-124-73-G88

National Aeronautics and Space Administration

U.S. Army Research Office-Durham

(NASA-CR-138226) EVALUATION OF MULTIBAND
PHOTOGRAPHY FOR ROCK DISCRIMINATION
(Colorado School of Mines) 119 p HC
\$8.75

CSCI 14E

63/14

N74-23047

Unclas
38384

May 1974

REMOTE SENSING PROJECTS

DEPARTMENT OF GEOLOGY

COLORADO SCHOOL OF MINES ♦ GOLDEN, COLORADO

EVALUATION OF MULTIBAND PHOTOGRAPHY
FOR ROCK DISCRIMINATION

By
Gary L. Raines

ABSTRACT

With the advent of the ERTS and Skylab satellites, multiband imagery and photography have become readily available to geologists. However, the direct application to geology of this multiband space imagery and photography and similar aircraft data has been somewhat hit-or-miss. In large part, this has been due to a lack of orderly, programmed multiband research and premature attempts to apply multiband remote sensing techniques directly to specific, complex, economic situations before their basic capabilities had been demonstrated on simple geologic problems. The fundamental research reported here examines one basic aspect of geologic remote sensing -- namely, the ability of multiband photography to discriminate rock variation. The concept evaluated is that narrow portions of the visible and photographic infrared spectrum, where reflectance differences occur, can be utilized to discriminate rocks by the use of multiband photography.

In order to take advantage of subtle reflectance differences, these differences must be recognized. Therefore, a simple filter wheel photometer (FWP) was designed for in situ measurement of band reflectances of the rock types to be discriminated. "Band reflectance" refers to the average spectral reflectance within a wavelength band, the width of which is defined by the transmission characteristics

of the filter under consideration. Thirteen bands were selected on the basis of filters suitable for multiband photography. The FWP is small, light, and costs less than \$200. Data acquisition is rapid, data reduction is simple, and all the spectral reflectance information needed for designing multiband photography can be acquired. The accuracy of the instrument when compared with standard techniques is good; the average error in band reflectance for most geologic targets is 20 percent and the precision is 3 to 5 percent.

Using the FWP, more than 8,600 in situ measurements of band reflectance of several sedimentary rocks were performed. The formations measured consist of carbonates, sandstones, and shales that are exposed in the Front Range of Colorado, mostly around Canon City, Colorado. From these 8,600 measurements, the following conclusions are drawn. The typical spectral reflectance curve for a geologic formation shows a gradual increase of spectral reflectance with increasing wavelength. The average band reflectance is about 0.20. Within a formation, the minimum natural variation is about 0.04, or about 20 percent of the mean band reflectance, and is commonly as high as 0.07, or 35 percent of mean band reflectance. The contrast ratio between formations (ratio of the band reflectances for two formations, calculated to give a number greater than 1.00) is generally less than 1.80, and between any two formations

the typical arithmetic difference between contrast ratios of different bands is 0.20. Statistical analysis shows it is necessary to have a minimum sample of 150 measurements per band per formation in order to select "best" film/filter combinations with differences of this magnitude, and in some cases, 300 measurements would be required. Therefore, "best" film/filter combinations cannot be selected, with acceptable statistical confidence, unless an impractical number of measurements is made.

At three test sites in the Colorado Front Range, the similarities of all band reflectances for a formation were tested. First, it is concluded that, for 13 bands, the mean band reflectance of a formation is statistically the same over a distance of 100 miles, although there are significant changes in the variance. Second, the conclusion concerning sample size is correct at all three sites.

Aerial multiband photography using various filter combinations was acquired using an International Imaging System (I²S) camera. All the photographs were processed to I²S specifications. These photographs were acquired in a manner that would allow for testing of the numerical conclusions and an evaluation of the numerous enhancement procedures that have been proposed.

Using this aerial photography, the numerical conclusions have been tested and evaluated. It is concluded from

analysis of this aerial multiband photography that (1) the differences in contrast ratios observed between all the filters considered are not statistically significant and (2) the spectral information in different bands is not advantageous. Therefore, because of the problem of getting multiple and simultaneously and correctly exposed photographs, the time involved in photographic manipulation, and the lack of statistically significant rock reflectance differences, the designed multiband photography concept for rock discrimination is not a practical method of improving sedimentary-rock discrimination capabilities. Concerning the general applicability of these conclusions, the formations considered have not been selected in a manner that would allow statistical inferences to be made about all rocks or even all sedimentary rocks. However, there is no geologic reason to suspect that the rocks and formations considered have unique reflectance properties. Therefore, the conclusions drawn apply in detail only to the formations considered; however, generalizations of conclusions are probably valid for most sedimentary rocks.

CONTENTS

	Page
Abstract.	iii
Introduction.	1
Purpose	2
Acknowledgements.	4
Test Site Geology	6
Phantom Canyon Subsite.	8
Harding Sandstone	9
Fremont Formation	10
Fountain Formation.	11
Dakota Group.	12
Niobrara Formation.	13
Pierre Shale.	14
Quaternary Deposits	17
Gorge Hills and Florence SE Subsites.	19
Kassler Test Site	19
Rock Reflectance.	21
Data Acquisition.	21
Equipment Design.	22
Operation	23
Accuracy and Precision.	27
Data Summary.	30
Rock Reflectance Properties	31
Extrapolation to Distant Areas.	40
Statistical Model	42
Implications of the Data.	42
Discussion.	48
Filter Selection.	53
Aerial Multiband Photography.	58
Photographic Data Analysis.	61
CAV Displays.	65
Evaluation of Aerial Multiband Photography.	71
Conclusions	76

	Page
Recommendation for Further Research	80
References Cited.	83
Appendix A: REDAT and REFLECT Computer Programs . . .	A1
Appendix B: Darkroom procedures for high-contrast, positive-negative MAC displays	B1
Appendix C: Explanation of photographic plates . . .	C1

FIGURES

	Page
Figure 1. Photographic example of filter selection. . .	3
2. Location maps of the test sites	7
3. Topographic profile and vegetation density profile	18
4. Filter wheel photometer system.	24
5. Passbands of filters.	25
6. Example of the graphical, data-reduction procedure for two filters	27
7. Plot of FWP band reflectance <u>versus</u> Munsell band reflectance.	29
8. Mean band reflectance and 80-percent confidence intervals for some of the Phantom Canyon data	32
9. Sample standard deviations for the Phantom Canyon data	33
10. Sample standard deviations for the Fountain and Fremont formations.	35
11. Use of the 80-percent confidence intervals.	37
12. Range of the contrast ratios observed at the Phantom Canyon Subsite.	38
13. Comparison between band reflectance measure- ments from the Kassler Test Site and the Canon City Test Site.	41
14. Definition of the min-max interval on the contrast ratio.	44
15. Normalized band reflectance	47
16. Effect of geologic expression upon selection of best filters	56
17. Diagram of the color additive viewer.	63
A1. Input data sheet for REDAT.	A1
A2. Input data sheet for REFLCT	A2
A3. Example of computer printout that is generated for each filter for each formation.	A4
A4. Computer-generated log reflectance plot	A5
A5. FWP data reduction flow chart	A6

TABLES

	Page
Table 1. Reflectance data for figure 1.	2
2. Statistical summary of two typical examples of FWP band reflectance data	36
3. Actual contrast ratios for the Phantom Canyon Subsite.	38
4. An example of the sample size calculation procedure used to determine the minimum sample size.	45
5. Relationship between sample size (n), standard deviation (s), the difference between mean contrast ratios (D), and the length of the interval on the contrast ratio (LCR).	45
6. Calculated band reflectance.	49
7. Phantom Canyon selection matrix.	54
8. The "best" filters and the formations discriminated "best"	55
9. Gorge Hills-Florence SE selection matrix . .	55
10. Best exposures for the filters considered. .	59
11. Cost of acquiring multiband photography (December, 1973)	60
12. Combinations of filters evaluated.	62
13. Inherent advantages and disadvantages of the Standard MB Combination in comparison with color and color infrared photography	66
14. Inherent advantages and disadvantages of the Standard B/W Combination in comparison with the Standard MB Combination.	68
15. Inherent advantages and disadvantages of the designed combinations in comparison with the Standard MB Combination.	68
16. Reflectance data and predictions concerning contrast of the Fountain and Lyons formations	69
17. Definition of color, CIR, and MAC displays .	70
18. Formation colors	78
B1. Supplies needed to make high-contrast, positive-negative masks.	B2

PLATES

Plate 1. Geology of the Canon City Test Sitesin pocket
2. Correlation of Formations.in pocket
3. Standard Multiband Combinationin pocket
4. Standard Black and White Combination and
Contrast Ratio Test Combination.in pocket
5. Phantom Canyon Designed Combination.in pocket
6. Gorge Hills-Florence SE Designed
Combination.in pocket
7. MAC Displaysin pocket

INTRODUCTION

Among researchers in remote sensing, the concept has developed that, by selection of the appropriate spectral band or bands of the electromagnetic spectrum, the tonal difference between targets can be preferentially enhanced so that targets are more easily discriminated. One particular application of this concept that seemed especially promising is multiband photography. Many geologists have proposed that multiband photography, with the appropriate selection of spectral bands in the photographic part of the electromagnetic spectrum (400-950 nanometers), is a means of obtaining increased tonal discrimination of rocks.

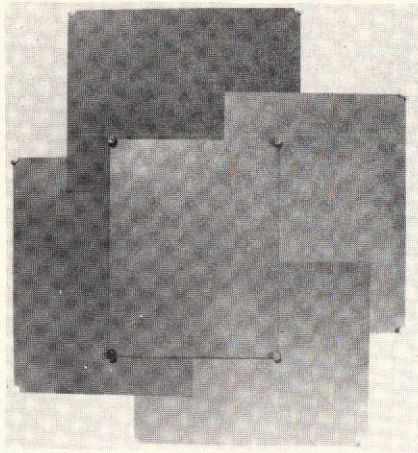
In geologic interpretations of aerial photography, the most significant recognition elements are texture, pattern, association of features, and tone (or color); lesser recognition elements are shape and size (Ray, 1960). Tone is an important aspect of all the recognition elements, since without tonal (or color) differences these other recognition elements would not be observed. Tone is defined as "each distinguishable shade variation from black to white" (Colwell, 1960). Therefore, tone (or color) is one of the most important aspects of discrimination and recognition of targets on a photograph.

Purpose

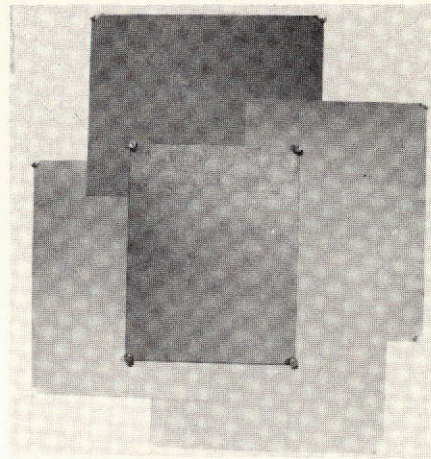
This research is an evaluation of the multiband photography concept that tonal differences between formations on aerial photography can be improved through the selection of the appropriate spectral bands. As an example of this multiband photography concept figure 1 is presented. Four matte-surface Munsell color cards with spectral reflectance curves were acquired from the Munsell Color Company, Baltimore, Maryland, and were photographed using Plus-X panchromatic film without a filter and with Wratten gelatin filters. "Spectral reflectance" is defined as the ratio of reflected radiant flux to incident radiant flux as a function of wavelength. If 20.5 percent of the incident radiant flux is reflected at a particular wavelength, the spectral reflectance at that wavelength is .205. "Band reflectance" is defined as the average spectral reflectance within a wavelength band. Table 1 shows the band reflectance for the color cards and for a Kodak 18 percent gray card that is used as a constant reference.

Table 1. Reflectance data for figure 1. The band names are filters, and the spectral bands (passbands) for each are given in figure 5 (p. 25).

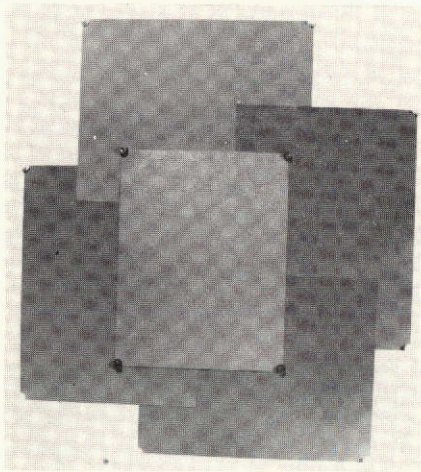
Munsell Color Card	Band Reflectance				
	No Filter	47B	15	22	92
5GY 5/6 (Moderate yellow green)	.138	.063	.186	.169	.142
5G 5/8 (Strong green)	.146	.118	.139	.095	.076
10B 5/6 (Moderate greenish blue)	.241	.343	.176	.156	.151
2B 5/6 (Moderate greenish blue)	.200	.234	.144	.116	.106
18% Gray card (Neutral gray)	.18	.18	.18	.18	.18



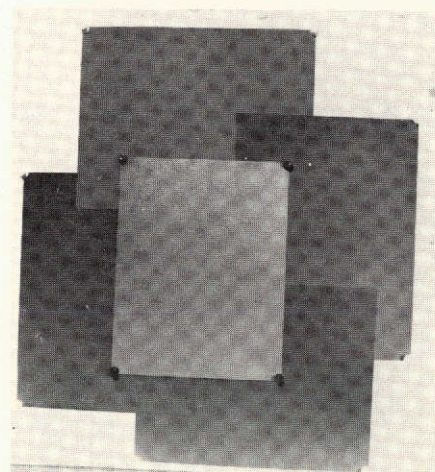
A NO FILTER



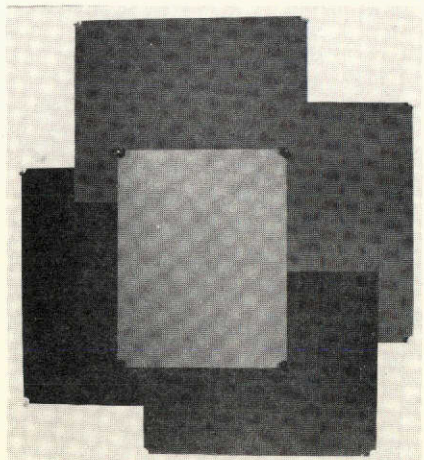
B WRATTEN 47B



C WRATTEN 15



D WRATTEN 22



E WRATTEN 92

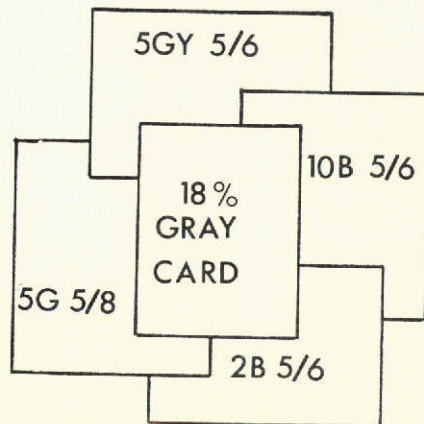


Figure 1. Photographic example of filter selection.

From inspection of figure 1 it can be seen that different colored cards are more easily discriminated with different filters (spectral bands) and that no single band is best for all the cards. Therefore, to achieve the best possible discrimination of all the cards, some combination of bands would be necessary. By analogy, the multiband photography concept for rock discrimination is: (1) to acquire band reflectance data for the rocks being considered, (2) to select the best combination of bands to discriminate the rocks using these reflectance data, (3) to acquire aerial photography using these selected bands, and (4) to extract the desired geologic information in an optimum manner.

Acknowledgements

This research was initiated with financial support from the Colorado School of Mines Bonanza Project (NASA Grant NGL-01-001-015), and the final three years of the research were financially supported by the U.S. Army Research Office-Durham (Grants DA-ARO-D31-124-71-G101 and DA-ARO-D31-124-73-G88). The advice and direction of my graduate committee, Doctors Keenan Lee (Chairman and Principal Investigator of the U.S. Army grants), Fred E. Moore, Richard H. De Voto, John O. Kork, and Frank C. Canney, and others is appreciated.

I especially would like to thank Dr. Keenan Lee for guidance and the supporting work performed. In addition I thank Ms. Kitty Huntley for typing and my wife for assistance and aiding with the editing of this dissertation.

TEST SITE GEOLOGY

In order to perform the evaluations proposed, two areas in Colorado (fig. 2) were selected as test sites. The Canon City Test Site was the primary test site where the major part of the work was performed. The Kassler Test Site, was selected in order to make an additional test of the conclusions and to evaluate the feasibility of using measurements from one area in a distant, geologically-similar area.

The Canon City Test Site was divided into three subsites. Dr. Keenan Lee made the reflectance measurements and geologic maps of the Gorge Hills area adjacent to Canon City, the Gorge Hills Subsite, and the area southeast of Florence, the Florence SE Subsite, and I made the reflectance measurements and geologic map of the area along the Phantom Canyon Road, the Phantom Canyon Subsite. These specific subsites were selected because the rock units characteristic of the Front Range (pls. 1 and 2) are well exposed in compact and accessible areas and the geology is simple, well-understood, and not complicated by faulting, folding, or significant lateral variation. The geologic map of the Phantom Canyon Subsite resulted from mapping by Brown (1963) and Gerhard (1964), and my photogeologic and field mapping of the bedrock geology; I mapped the Quaternary deposits using combined photogeologic and field methods.

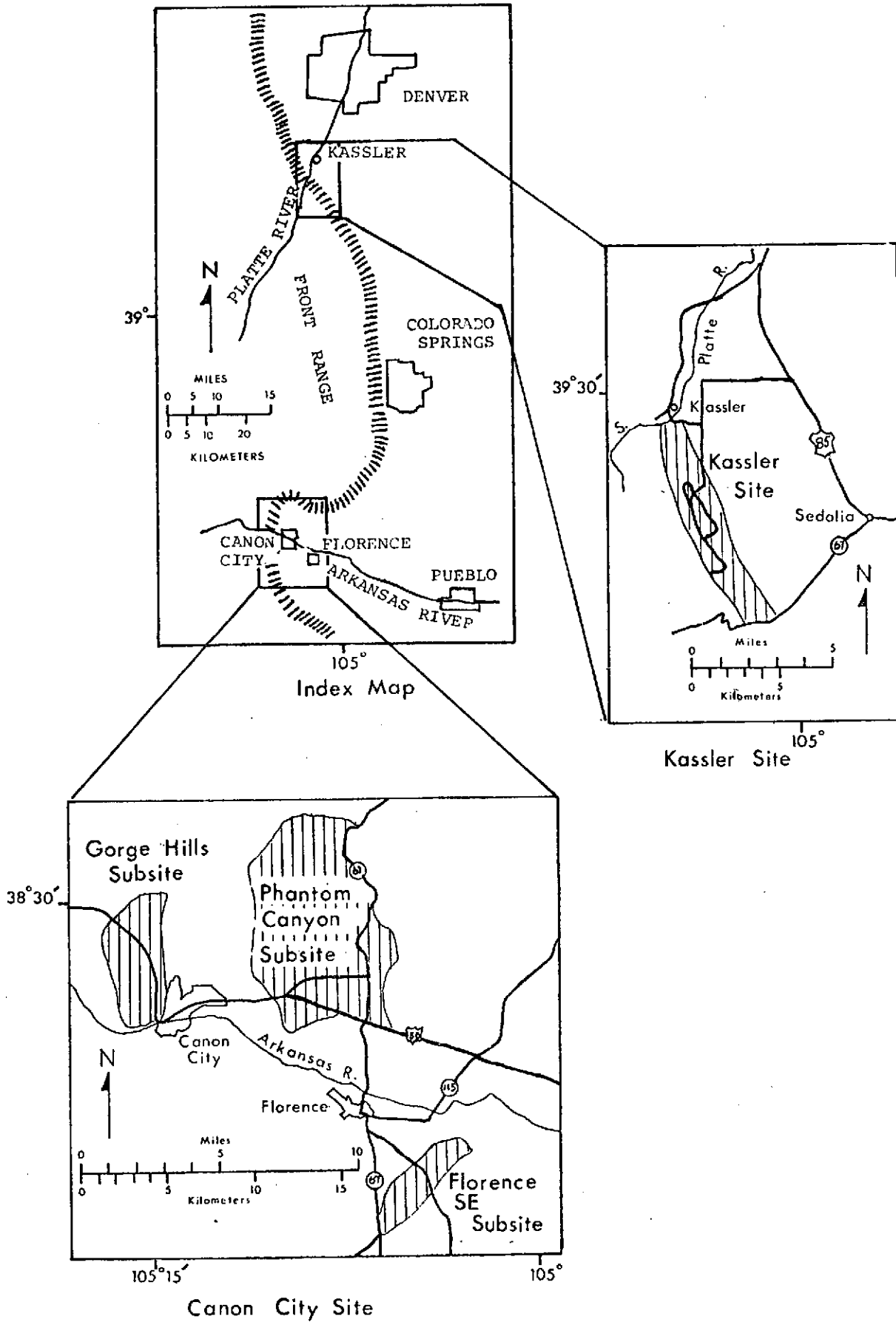


Figure 2. Location maps of the test sites.

The geologic maps of the Gorge Hills and Florence SE subsites were compiled, checked, and modified by Dr. Keenan Lee from work by Webster (1959) and Mann (1957). Further geologic details on the Canon City Test Site can be found in Tolgay (1952), Saylor (1955), Robertson (1957), Ogden (1958), Brady (1958), Warren (1960), Sackett (1961), Cramer (1962), Lucken (1964), and Gerhard (1961 and 1967).

The Kassler Test Site was selected because it is similar to the Canon City Test Site, it is readily accessible, and bedrock and surficial geologic maps are available (Scott, 1963a, 1963b).

In the following sections the geology of the subsites is briefly described. The Phantom Canyon Subsite is described in greatest detail, since this is the area studied most extensively, and it is not different in pertinent factors from the other test sites.

Phantom Canyon Subsite

The Phantom Canyon Subsite consists of sandstones, shales, and carbonates with a discontinuous cover of Quaternary alluvium on a Precambrian igneous and metamorphic basement complex. The structure is comprised essentially of gentle- to moderate-south-dipping formations with east-west faults repeating the Paleozoic rocks.

The stratigraphic section of the Phantom Canyon area is depicted in plate 2, and plate 1 is a geologic map showing the distribution of these units. Due to the degree of exposure and covering by Quaternary material, the only bed-rock units considered are the Harding Sandstone, the Fremont Formation, the Fountain Formation, the Dakota Group, the Niobrara Formation, and the Pierre Shale. The formations above and below these units are dealt with in only a general way.

Harding Sandstone - The Harding Sandstone (Walcott, 1892; Gerhard, 1967) crops out in moderately extensive south-dipping dip slopes and on steep anti-dip slopes below the Fremont Formation in the northern part of the map area. In a fresh hand specimen the rock is generally a white bimodal, well-sorted, well-cemented quartz sandstone in the upper and lower parts of the formation. The cement is generally siliceous and the sand grains are frosted. The central part of the formation is generally a very poorly exposed, red and green shale. On weathered outcrops and dip slopes the formation is variegated reds, greens and whites; however, the dominant color is a pale reddish brown to a moderate reddish brown (10R 5/4 to 10R 5/5). Trace fossils, fish plates of ostracoderms, and other fossils believed to be Champlainian in age (Brainerd and others, 1933; Fischer, 1973) are characteristic of this formation. Gerhard (1967)

reports the formation ranges in thickness from approximately 20 to 100 feet from south to north in the map area. The Harding Sandstone in this area is bounded by angular unconformities showing moderate relief, with the Manitou Formation below and the Fremont and Fountain formations above. In the northeastern part of the area (secs. 4, 5, 8, and 9, T. 18 S., R. 69 W.), the Fremont Formation was never deposited or it was eroded by pre-Fountain time erosion and the Harding Sandstone is overlain by the Fountain Formation. This area with the Fountain Formation resting on the Harding Sandstone is fault-bounded and extends several miles east of the map area. Wherever the Harding Sandstone is still capped by the Fremont Formation, the uppermost part has a yellow sandstone that is very distinctive in cliff exposures.

Fremont Formation - The Fremont Formation (Walcott, 1892; Gerhard, 1967) crops out as extensive south-dipping dip slopes in the northern part of the map area. In fresh hand specimen the rock is a pale red (10R 6/2), fine to coarse crystalline, fossiliferous dolomite. Chert nodules forming highly irregular, discontinuous zones are very common. The fossils consist predominantly of broken and scattered crinoid stems. On the weathered surface of the outcrop the color is a grayish orange pink (YR 7/2) to

a pale red (10R 6/2), with the dominant color closer to grayish orange pink. The thickness of the formation is variable due to the development of a karst topography before deposition of the Fountain Formation, and due to non-deposition (Monk, 1954). The thickness ranges from zero to 90 feet (Gerhard, 1967). The Fremont Formation is bounded by angular unconformities with the Fountain Formation above and the Harding Sandstone below. Sweet (1954) considers the Fremont to be of Cincinnati age, where Brainerd and others (1933) believe that it represents Trentonian and part of Richmondian time.

Fountain Formation - The Fountain Formation (Cross, 1894; Gerhard, 1964) crops out in extensive south-dipping dip slopes and in small stream cuts in Eightmile Park. The lithology of the formation is extremely variable. The lower part is composed of coarse, arkosic, conglomeratic sandstone beds and siltstone seams. The upper part generally is covered by Quaternary gravels; however, exposures in stream channels show that it is composed of non-resistant, fine- to coarse-grained-sandy shale. The colors of the formation are whites and reds; however, the dominant color is dark reddish brown (10R 3/4). Internally, the Fountain Formation consists of numerous cut-and-fill deposits. In the map area the Fountain Formation is 1,200

feet thick (Maher, 1953). The lower contact of the Fountain Formation is an angular unconformity with the Fremont Formation or the Harding Sandstone. Where the Fountain Formation overlies the Fremont Formation, Fountain material can be seen to fill the karst topography developed in the Fremont Formation. The upper contact is probably gradational with the overlying Lykins Formation (Gerhard, 1967).

Calamites (?) was found in the NE $\frac{1}{4}$, sec. 8, T.18 S., R. 69 W. The exact age of the Fountain Formation is difficult to determine due to lack of diagnostic fossils. Hubert (1960) interpreted the Fountain to be Atokan through Virgilian and possibly including Wolfcampian and early Leonardian; Meher (1953) believes that it represents Atokan through Missourian and possibly Virgilian.

Dakota Group - The Dakota Group (Meek and Hayden, 1862; Brown, 1963) crops out as an extensive south-dipping hogback in the central part of the map area. The formation consists of an upper and lower massive, cross-bedded, poorly sorted sandstone with numerous, thin shaley layers. The middle part of the formation is a poorly exposed, sandy, carbonaceous shale often with a blocky weathering habit. On the weathered surface of the outcrop the color of the upper Dakota Group is a yellow red (5YR variable); however the color of the outcrops is greatly modified by the common

occurrence of lichen covering giving the outcrops a color from yellow red to greenish yellow (5YR to 5GY variable). The thickness of the formation is approximately 300 feet. The lower contact of the Dakota Group is gradational with the Morrison Formation and is generally not exposed due to landslides. The upper contact is gradational with the Benton Group. The age of the Dakota Group is Early Cretaceous.

Niobrara Formation - The Niobrara Formation (Meek and Hayden, 1862; Brown, 1963) is composed of two members: the Fort Hays Limestone Member and the Smoky Hill Shale Member (Mudge, 1877; Williston, 1893; Cragin, 1896; Brown, 1963; Scott and Cobban, 1964).

The Fort Hays Limestone Member crops out on a low hogback across the southern part of the map area. The member consists of light-gray, fossiliferous, argillaceous limestone beds generally about one foot thick, interbedded with light-gray shale seams up to one inch thick.

Inoceramus are very common, especially I. labiatus. The thickness of the member along Sixmile Creek (sec. 21, T. 18 S., R. 69 W.) is approximately 60 feet. The lower contact is conformable with the Juana Lopez Member of the Carlisle Shale of the Benton Group (Scott, 1969). The upper contact is gradational with the Smoky Hill Shale. The age of the Fort Hays Limestone at Pueblo, 50 miles east of

the map area, is late Turonian and early Coniacian (Scott, 1969).

The Smoky Hill Shale exposures are in an area of little relief in the southern part of the map area. The lowest part of the member includes some low limestone hogbacks. Possibly these areas have such low relief because they were beveled off, and the surficial material was reworked by the Piney Creek episode of terrace building. In stream cuts the Smoky Hill Shale consists of light-gray, calcareous shale that often has a blocky weathering habit. Scott and Cobban (1964) divided this member into seven units on the basis of the ratio of shale to limestone; however, due to the limited and poor exposures, these subdivisions were not made for this study. The thickness of the Smoky Hill Shale, determined from cross sections, is 340 feet. The lower contact of the member with the Fort Hays Limestone is gradational and the upper contact is gradational with the Pierre Shale. The upper contact as mapped is the top of a sometimes-prominent yellow-orange calcareous shale zone. Scott (1969) reports numerous fossils in the Smoky Hill Shale Member and states the age of the member at Pueblo, Colorado, as Coniacian, Santonian, and early Campanian.

Pierre Shale - The areas of the Pierre Shale (Meek and Hayden, 1862; Brown 1963; Scott, 1969; Gill and others, 1972) are characterized as low, rolling topography in erosional

windows in the southern-most part of the map area. For the purposes of this study the formation was informally subdivided into seven units that are mappable in this part of the Canon City embayment. The units are, from base up, (1) the AB unit, consisting of the transition member (Scott, 1969), the Apache Creek Sandstone Member (Lavington, 1933; Scott and Cobban, 1964; Scott, 1969), and the Sharon Springs Member (Elias, 1931; Scott, 1969), (2) the Rusty zone of Gilbert (1897) (Scott, 1969), (3) the lower Tepee zone consisting of the lower part of the "tepee buttes" zone of Gilbert (1897) (Scott, 1969), (4) the upper Tepee zone consisting of the upper part of the "tepee buttes" zone of Gilbert (1897) (Scott, 1969), (5) unit C, (6) unit D, and (7) the upper transition unit. The primary mappable features that have been used to distinguish these units are the following. The uppermost part of the AB unit, the Sharon Springs Member, is a resistant shale, commonly with a blocky weathering habit and large septarian concretions. Vegetation is very sparse on this member. The Rusty zone is mantled with ironstone concretions that have weathered out of discontinuous lens-like zones. Septarian concretions are more common in the upper part, which is gradational with the lower Tepee zone. The lower Tepee zone lacks the ironstone concretions and has "tepee buttes" (described by Scott, 1969) in the uppermost part. The upper Tepee zone

is like the lower Tepee Zone with the addition of several thin limestone beds. The C unit is a prominent ridge-forming shale that has cone-in-cone structures along the ridgetop. The D unit is a non-resistant, poorly exposed shale with yellow-orange, sandy concretions in the upper part. The upper transition unit is a calcareous, fine-grained-sandy shale. Numerous discontinuous finely laminated to thin-bedded, shaley sandstones form low hogbacks.

This Pierre Shale section has been measured (Gill and others, 1972) and biostratigraphically zoned (Scott, 1972, personal communication), and most of the details of the section are from those studies; however, the units mapped are my own subdivisions. Plate 2 summarizes the stratigraphy of the Pierre Shale. The units as described generally have gradational lithologic changes that result in minor topographic and geomorphic features that greatly aid mapping. These units are easily mapped along the Phantom Canyon Road (secs. 21, 28, and 33 and E½ secs. 20, 29, and 32, T. 18 S., R. 69 W.) and can be mapped in another erosional window on the Colorado State Prison Farm (sec. 31, T. 18 S., R. 69 W.). The area between the Phantom Canyon Road and the Prison Farm has a discontinuous cover of Quaternary gravel that makes mapping of the subdivisions of the Pierre Shale very difficult.

While mapping the Pierre Shale at Phantom Canyon and the Prison Farm, it was found that the density of several

plants could be used for geologic mapping. Figure 3 shows an exaggerated topographic profile approximately north-south across the Pierre Shale with plant-density data. A point-step method (Miller, R.F., 1972, personal communication) averaging the number of plants over approximately 60 feet was used to quantify the vegetation density. The point-step method consists of marking a point on the toe of one's right boot and then pacing across an area. For each pace of the right boot whatever the point on the boot comes down on is recorded and summed over ten paces. For this study, only certain plant species and total density were recorded. The vegetation studies concentrated upon the larger shrubs, which are very useful in the field and can be of some assistance when working with aerial photography of an appropriate scale. Soil moisture studies and whole-rock, emission-spectrographic analyses were performed in an attempt to explain why the vegetation changes observed on figure 3 occur. No satisfactory explanation could be found.

Quaternary Deposits - Quaternary deposits consisting of pediment gravels, terrace gravels, colluvium, and alluvium cover extensive areas. These deposits were mapped where they include enough transported material to make their surface appearance different from that of the bedrock. The work done with these deposits consisted of mapping their

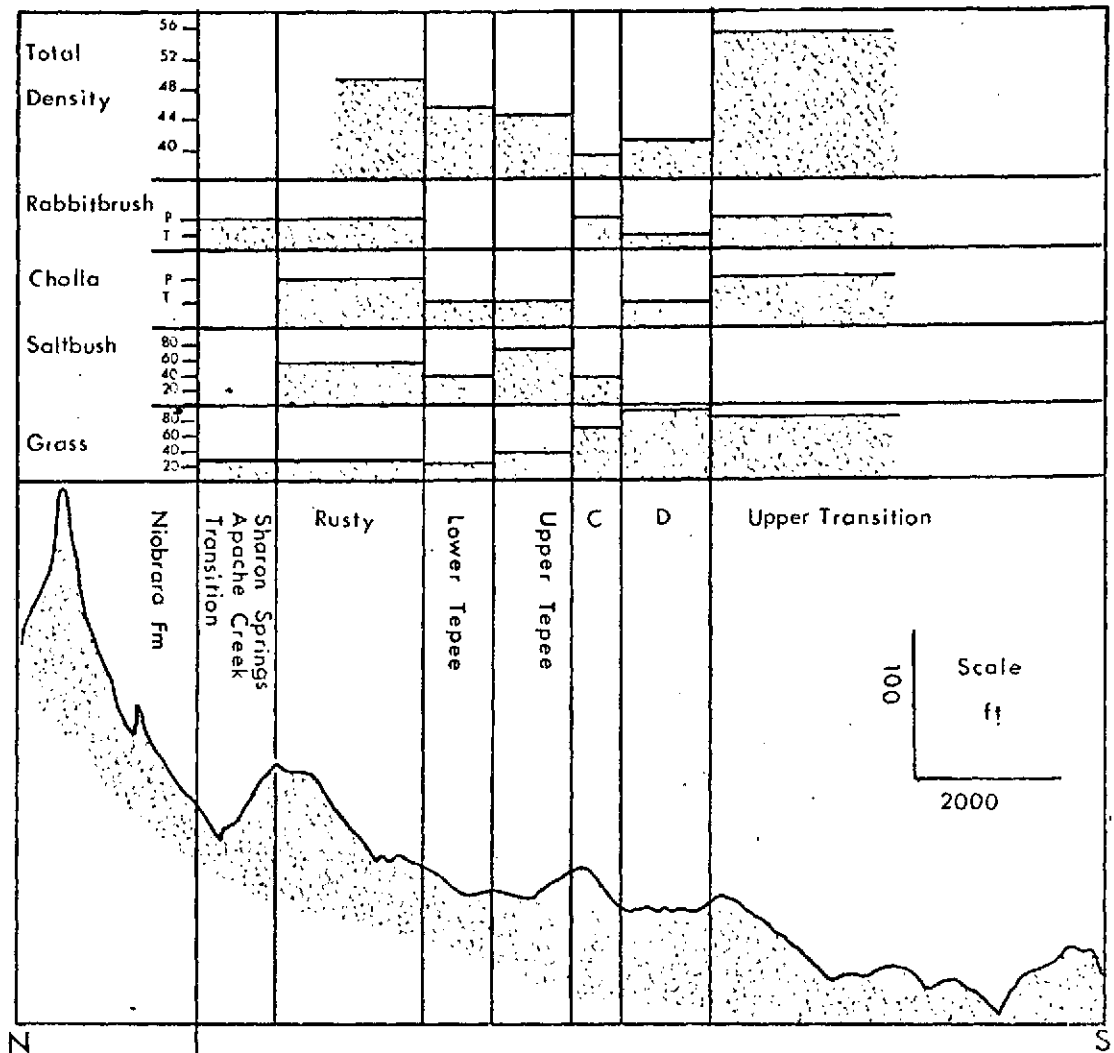


Figure 3. Topographic profile and vegetation density profile. Total density is percent of ground coverage. For saltbush and the grasses the units are percent of the total vegetation community. For rabbitbrush and cholla, P means the plant is present but so dispersed that it is not well-recorded by the point-step method, and T means the plant is present but fewer individuals than P. The proper names for the plants considered are rabbitbrush (*Chrysothamnus nauseosus* (Pall.) Britt.), cholla (*Opuntia imbricata* (Haw.) DC.), saltbush (*Atriplex confertifolia*), grasses (various types). The profile is oriented north-south through secs. 21, 28, 33, T. 18 S., R. 69 W., of the Phantom Canyon Subsite.

distribution, making a reconnaissance survey of lithologies, noting their height above modern streams, and correlating this information with Scott (1969) in order to suggest names for the deposits. The suggested correlations are considered tentative (See plate 1 for the distribution and suggested correlations).

Gorge Hills and Florence SE Subsites

The Gorge Hills and Florence SE subsites were included in this study because (1) they are near the Phantom Canyon Subsite, (2) the same bedrock units are exposed, and (3) they can therefore be used for comparison of procedures and results derived at the Phantom Canyon Subsite. Plates 1 and 2 include maps and the columnar sections of the Gorge Hills and Florence SE subsites. These areas are considered sufficiently similar to provide areas to test the conclusions derived at the Phantom Canyon Subsite.

Kassler Test Site

The Kassler Test Site was selected because (1) the same bedrock units are exposed as at the Canon City Test Site, except for the pre-Pennsylvanian section, (2) it is remote from Canon City (fig. 2), and (3) the bedrock and surficial geology has already been mapped (Scott, 1963a,

1963b). However, the Pierre Shale cannot be observed on aerial photography because of Quaternary material so this unit was not included in this study. A stratigraphic section is shown on plate 2. For more details of the geology and geologic maps of the area the reader is referred to Scott (1963a, 1963b). From stratigraphic information in plate 2, limited field work, and Scott's reports, it is concluded that the Kassler Test Site is sufficiently similar to the Canon City Test Site to provide areas to test the conclusions derived at the Canon City Test Site.

ROCK REFLECTANCE

Multiband photography is a remote sensing technique that attempts to take advantage of subtle, spectral reflectance differences between several targets in order to produce enhanced target discrimination on the resultant photography. The first step in the design of multiband photography is to select a set of spectral bands that are optimum for the discrimination of the formations considered. To accomplish this, the spectral reflectance properties of the formations must be measured and then analyzed to select the best set of spectral bands. This section describes how these measurements were obtained, summarizes the measurements, and discusses some implications.

Data Acquisition

Initially, various spectroradiometers were considered for field-data collection, and an Instruments Specialty Company (ISCO) instrument was selected and used. The ISCO spectroradiometer is a continuously scanning instrument sensitive from 380 to 1550 nanometers. A fiber optics bundle with a diffusing screen having a 180° field of view and cosine response is used to transmit light to the detector. The ISCO and its chart recorder can be operated by a 12-volt automobile battery and is fairly portable when used with a

vehicle. The ISCO spectroradiometer, without the chart recorder, is self-contained with internal batteries and can be transported easily by backpack. However, the amount of data that has to be recorded when using the ISCO without the chart recorder makes the measurement procedure very tedious and time-consuming. In addition, the data reduction problems rapidly become overwhelming.

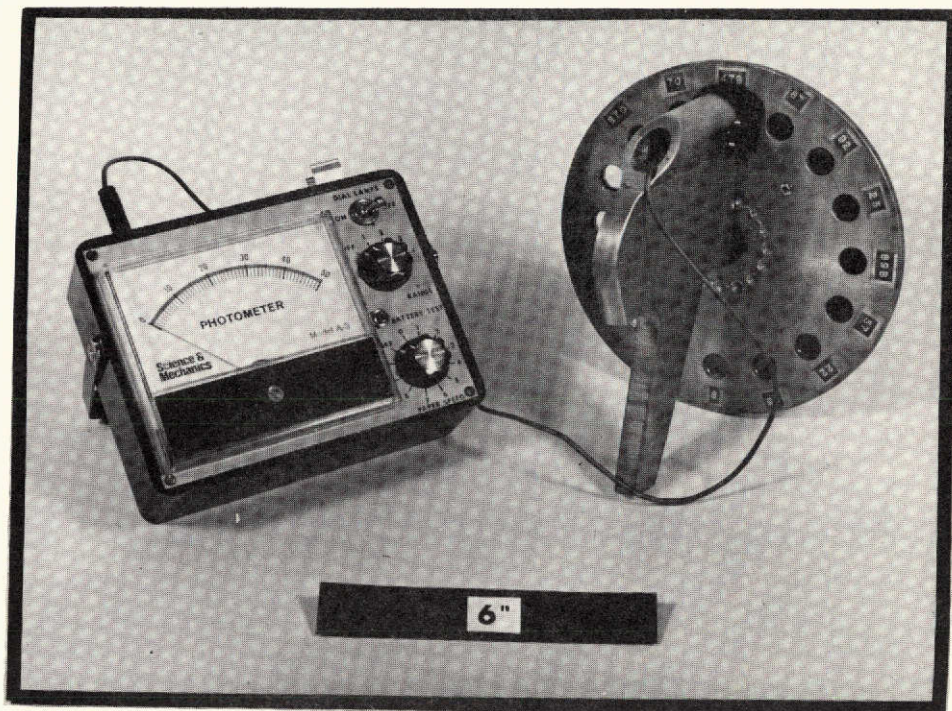
To overcome these problems and to make measurements in remote areas, a filter wheel photometer (FWP) modified after Egbert and Ulaby (1972) was designed, built, and used in the course of this research. Figure 4 illustrates the FWP. This instrument is small, light, and costs less than \$200. Data acquisition is rapid, data reduction is simple (although still time-consuming), and all the spectral reflectance information needed for designing aerial multi-band photography can be acquired.

Equipment Design - The FWP consists of two parts: a very sensitive photometer and a holder for the filters. The photometer used is manufactured by Science and Mechanics and is a very sensitive, darkroom light meter using a cadmium-sulfide detector. The spectral sensitivity of the instrument is sufficiently broad to cover the full photographic range. Knowledge of the exact spectral sensitivity of the instrument is not needed, since the

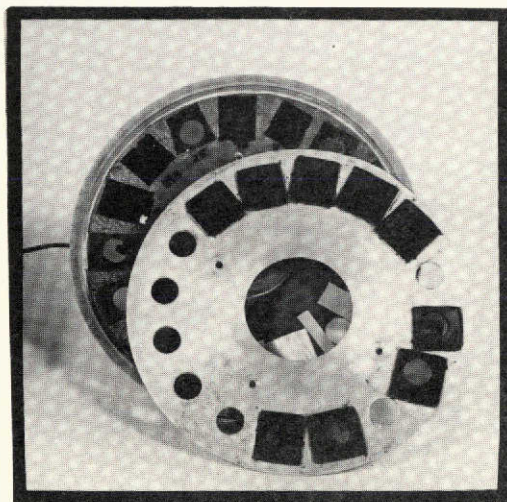
instrument is calibrated in use with known standards as discussed below.

The holder for the filters consists of a pistol grip with a rotatable wheel attached (fig. 4), with the photometer probe in the grip behind the filter wheel. The wheel has 16 circular holes over which the filters (or filter sandwiches) are placed. Filters are mounted on a plastic plate on the filter wheel so that they can be changed easily. Up to sixteen filters can be used. By loosening three screws, the plastic plate can be exchanged for another. Thus, the number of filters that can be used is limited only by measurement time and filter availability. For the purpose of this research, Wratten gelatin filters that could be used for aerial multiband photography were selected. The passbands of the 13 filters used are shown in figure 5. The field of view of the FWP is variable, depending on the positioning of the photometer probe; however, as normally used, the field of view is about 10° .

Operation - The operation of the FWP in the field is very simple and rapid. A small, portable, voice tape recorder is used to record notes and data, thus allowing one person to easily operate the FWP. In addition to the FWP, a set of calibration standards of known reflectance is needed. For calibration measurements, an 8-inch by



A



B

Figure 4. Filter wheel photometer system. Rear view (A) shows how the filters are distributed. Front view (B) shows the front plate removed with glass, infrared blocking filters (Corning 3961) and the internal plastic plate with Wratten gelatin filters.

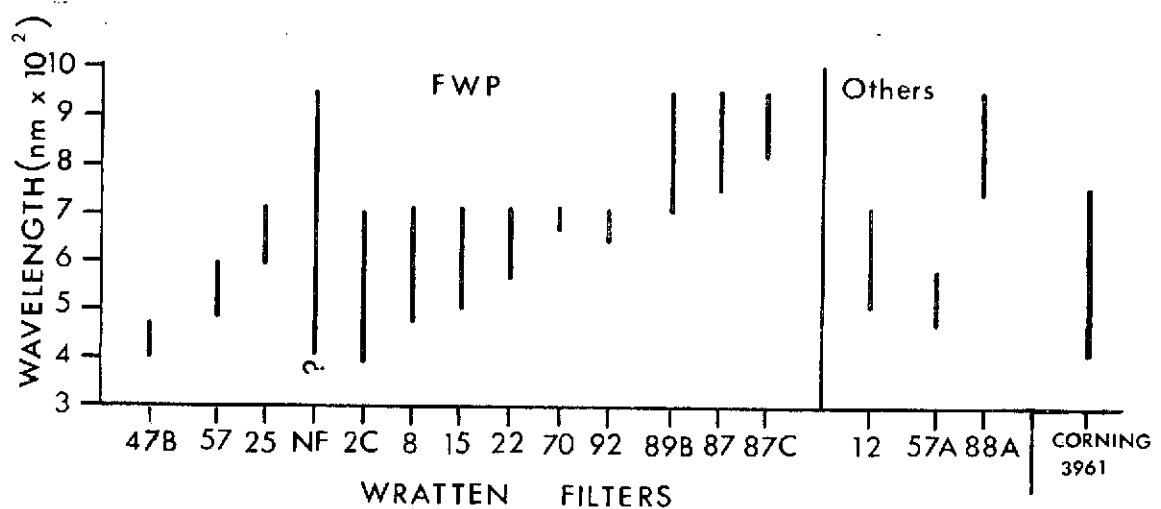


Figure 5. Passbands of filters. All of the filters are Wratten gelatin filters. All the filters except the 87, 87C, 88A, 89B, and NF are used with an infrared blocking filter (Corning 3961). NF means no filter and is therefore not a filter; however, for convenience of terminology the NF spectral band will be referred to as a filter. The passband is defined by the wavelength interval with greater than 10 percent transmission. Other filters refers to filters not used with the FWP but referred to in the text.

11-inch, Kodak 18 percent gray card and two Munsell gray cards, N 3.5/ and N 6.5/, with reflectances of about .06 and .40, respectively, are used. These standards are measured in the laboratory by the Munsell Color Company with standard laboratory equipment.

The field measurement procedure is as follows:

- 1) Place the calibration standards on a piece of black cloth in an orientation relative to the sun that is the same as the surface to be measured.
- 2) Hold the FWP with the photometer probe vertically over the calibration standard such that the

standard fills the field of view, and make measurements by rotating each filter in front of the photometer probe and recording the meter value.

- 3) Hold the FWP probe vertically over the target surface to be measured and repeat the measurements with each filter. Generally, several targets may be measured before the standards are measured again, depending upon the stability of the atmosphere.
- 4) Measure the calibration standards again with each filter.

By following this procedure with the FWP, it takes about two minutes per target to make and record 13 spectral measurements.

The data reduction can be done graphically, or it can be programmed and done by computer. The graphical technique consists of plotting the known calibration-standard measurements (band reflectance versus meter reading) on a graph, with meter reading as the abscissa and band reflectance as the ordinate, fitting a line to the plot, and then reading the target band reflectance from this curve (fig. 6). Band reflectance refers to the average spectral reflectance within a wavelength band, the width of which is defined by the transmission characteristics of the filter under consideration.

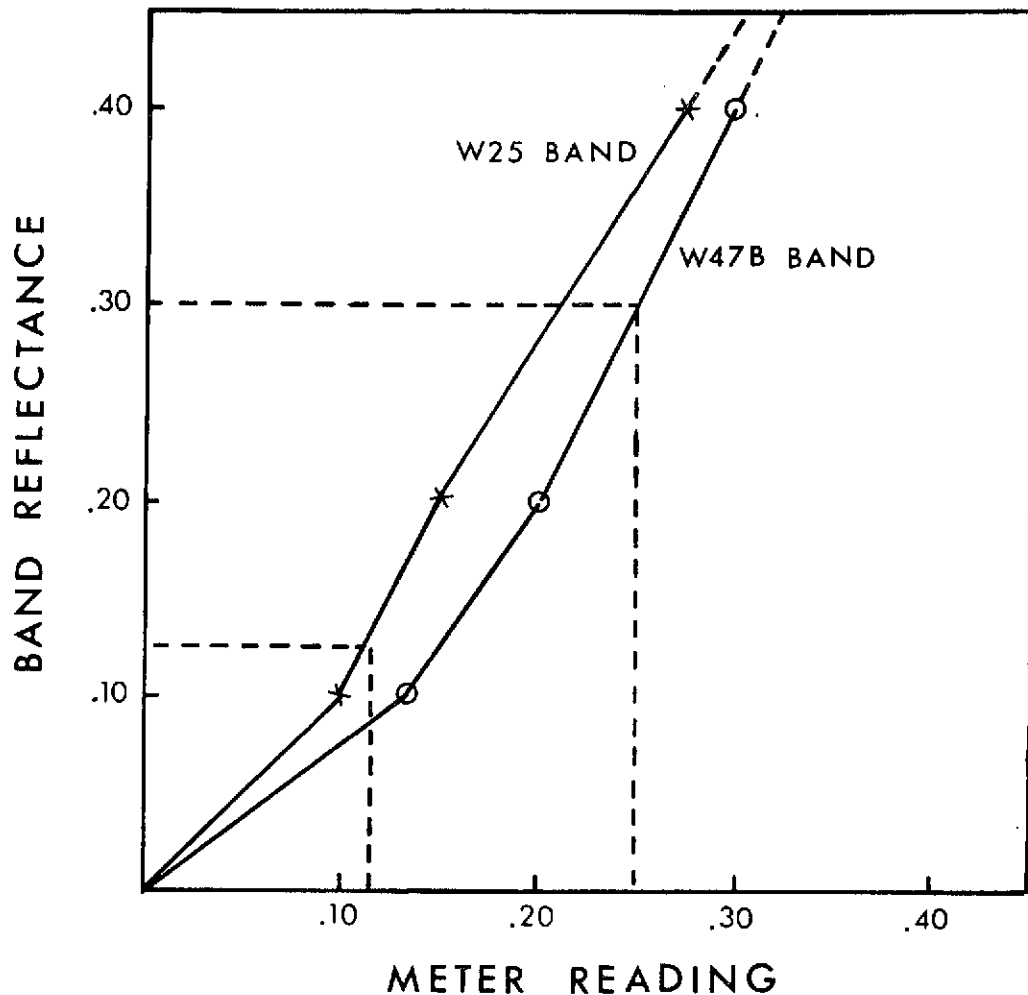


Figure 6. Example of the graphical, data-reduction procedure for two filters. The circles (o) and cross (+) are points obtained from the calibration standards. The dashed lines give an example of a target measurement for each band. The computer program to do this calculation is called REDAT, described in Appendix A.

Accuracy and Precision - Several tests of the accuracy and precision of the FWP have been made, and the FWP measurements agree well with those from standard-measurement procedures. The tests consisted of measuring colored Munsell standards (8-inch x 11-inch, matte surface) under field

conditions. The spectral reflectance curves for the colored standards used were originally derived by the Munsell Color Company, using a spectrophotometer with the sample diffusely illuminated by a tungsten-halogen light source and viewed at an angle of 8° from the normal. The specular component of the reflection was included, but this is of little importance in the measurement of matte-reflecting samples. The white reflectance standard used was Zeiss BaSO_4 , which has a reflectance of about .985 for the visible part of the spectrum (David H. Alman, 1973, personal communication). These continuous, spectral reflectance curves were then integrated over the pass band intervals for the filters under consideration (between the 10-percent transmission points). Then a plot of these Munsell band reflectance values versus the FWP band reflectance values was made (fig. 7).

Several Munsell standards were used to provide a range of reflectance values (from .06 to .40) for each filter. The Munsell standards used were 2.5B 5/6, 10B 5/6, 5GY 5/6, and 7.5R 5/6. Linear correlation coefficients were calculated for each standard, and they ranged from .83 for the 2.5B 5/6 standard to .95 for the 10B 5/6, showing the greatest accuracy near a band reflectance of .20. For all standards combined, the grand linear correlation coefficient was .81; and with 40 observations, it can be said with 99.9-percent confidence that a linear

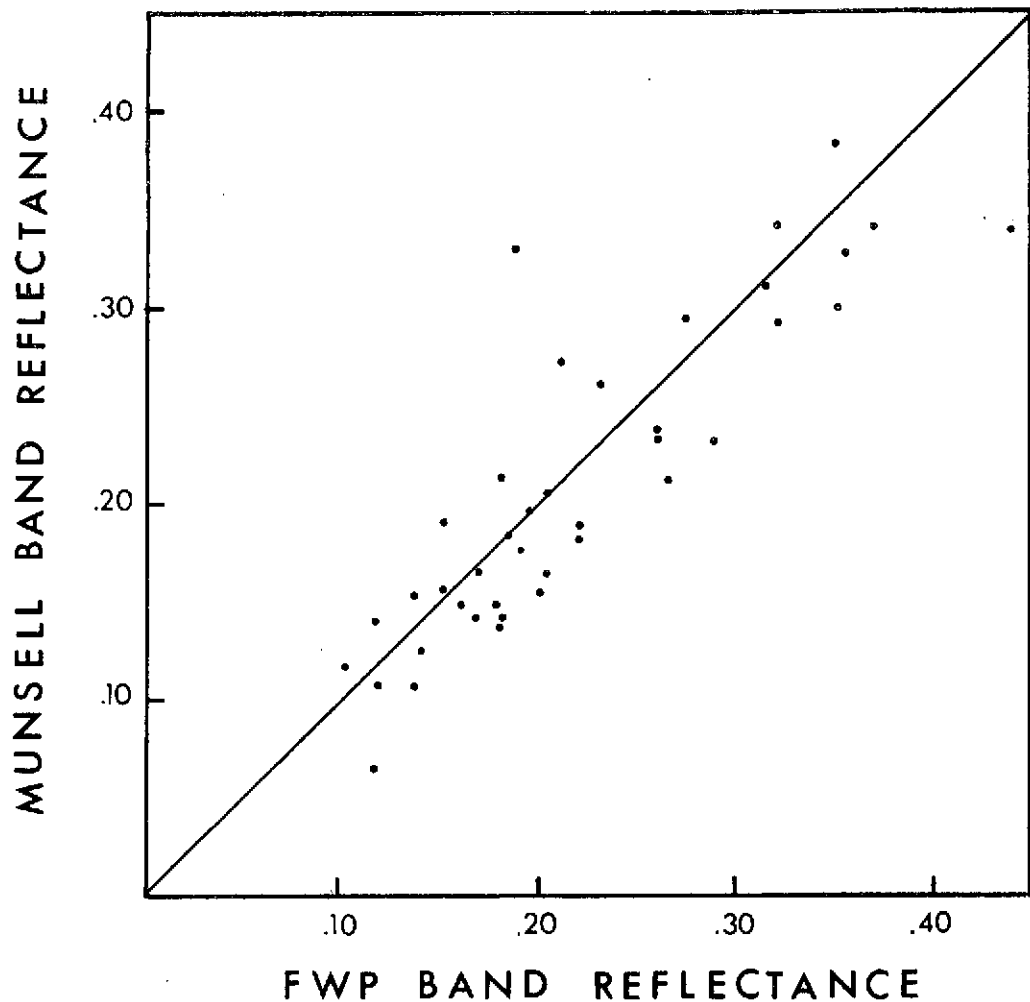


Figure 7. Plot of FWP band reflectance versus Munsell band reflectance. The line represents perfect accuracy.

relationship exists. The average error in accuracy of the FWP band reflectance measurements is .039, where

$$\text{average error} = \sqrt{\frac{\sum_i [(FWP - M)^2]}{n-1}}$$

FWP = FWP measurement for observation i , $i=1, \dots, n$

M = Munsell measurement for observation i

n = sample size

For the average band reflectance of .20 the corresponding error is about .04; therefore, the accuracy of the FWP is 20 percent.

In a similar manner, the precision of the FWP was found to be approximately ± 0.01 , or 3 to 5 percent of the average band reflectance. The precision test was conducted in the field under working conditions by making repetitive measurements on a colored Munsell standard; therefore, part of the precision error is due to variability of the atmospheric conditions, which is uncontrollable.

Data Summary

In the course of evaluating the capabilities of multiband photography to discriminate rocks, more than 8,600 in situ measurements of band reflectance of 23 sedimentary formations were acquired. Dr. Keenan Lee made all of the band reflectance measurements at the Gorge Hills and Florence SE subsites and I made all the band reflectance measurements at the Phantom Canyon Subsite and the Kassler Test Site.

The purposes of this section are to (1) summarize these measurements, (2) note generalizations that are of interest to remote sensing researchers working with the visible and photographic infrared parts of the spectrum (400 to 950 nanometers), and (3) give generalized parameters for a

statistical model of rock reflectance. Then, using the data presented, the sample size requirements for use of these types of data are discussed. Specifically, data on the amplitude variation of the mean band reflectance between formations, and the natural variability of band reflectance within a formation, are discussed. Computer plots of all 8,600 measurements can be obtained through the Geology Department, Colorado School of Mines, Golden, Colorado 80401.

Rock Reflectance Properties - Typical band reflectance measurements made at the Phantom Canyon Subsite are presented in figure 8 which shows the mean band reflectance for each formation and an 80-percent confidence interval for the mean, generally for a sample size of 12 measurements per band per formation. From inspection of figure 8 band reflectance in this part of the spectrum (400 to 950 nanometers) offers little opportunity for unique identification by use of the spectral character.

The standard deviation is an estimate of the variability of the reflectance data, and a summary of all the standard deviations observed is shown in figure 9. Variability includes variation due to random error, measurement errors, and atmospheric-condition and natural-target variability. The variation due to random error and measurement procedure is 3 to 5 percent of the mean band

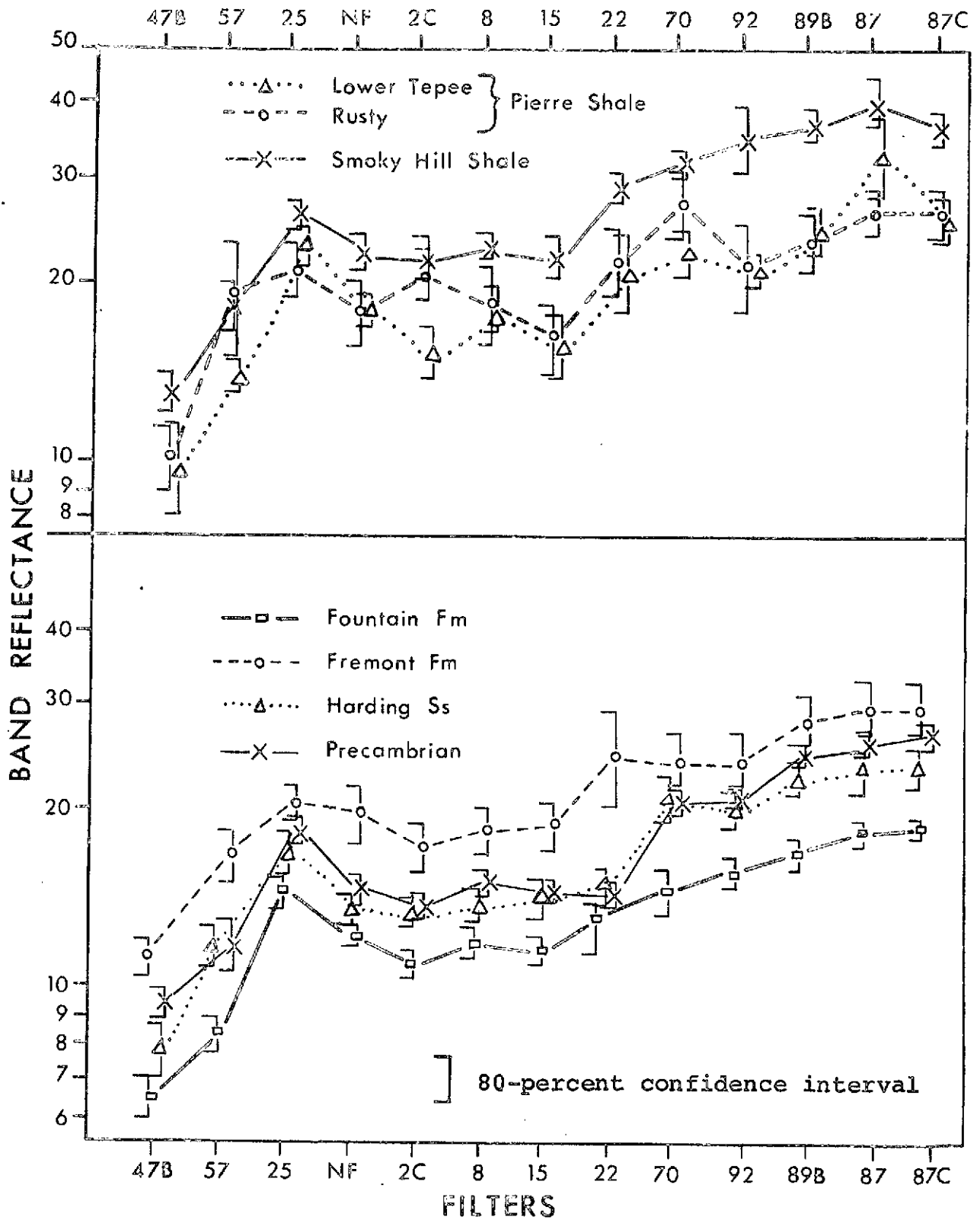


Figure 8. Mean band reflectance and 80-percent confidence intervals for some of the Phantom Canyon data. The lines connecting the points are to aid visualization only. Formations are listed in stratigraphic order.

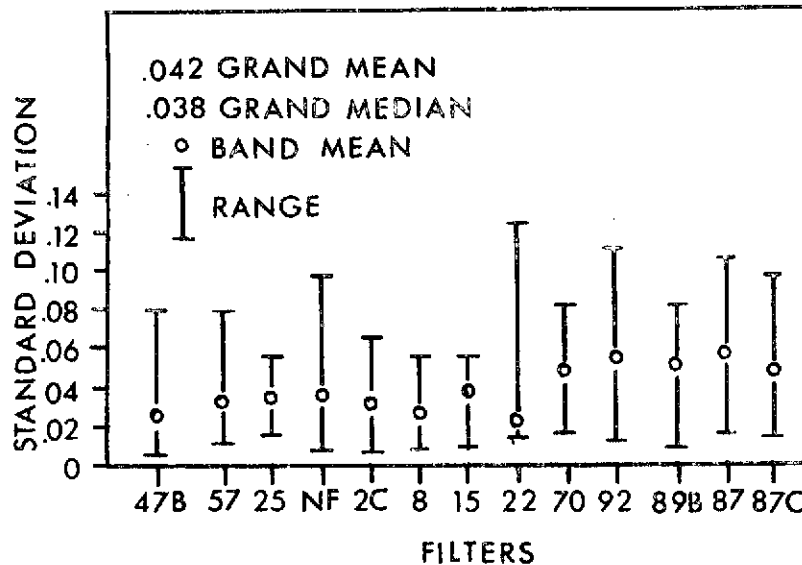


Figure 9. Sample standard deviations for the Phantom Canyon data. Eighty-five percent of the observed standard deviations are less than .07.

reflectance; thus the observed variation is primarily due to natural variability.

The grand mean of all the standard deviations is .042 band reflectance, and analysis of the range shows that 85 percent of the observed standard deviations are less than or equal to .07. The grand median of the standard deviations is .038. The significance of these standard deviations is best assessed by realizing that the grand-mean band reflectance, using all the data, is approximately .20. Therefore, the grand mean standard deviation (.042) is about 20 percent of the grand mean of the mean band reflectances. Furthermore, the procedure used in the field was to measure "typical" areas; therefore, the mean standard deviation (.042) is a minimum estimate of the

variation. Thus, for a single formation, the data indicate very significant variation of the band reflectance within a formation.

In order to delimit further the population standard deviation, the Fremont Formation and the Fountain Formation were selected, and respectively, 62 and 39 band reflectance measurements per band were made. More measurements were desired; however, due to time and weather problems, more measurements were not obtained. For measurements of the Fremont and Fountain formations, variation of band reflectance within the formation specifically was sought, in order to acquire an estimate of the maximum standard deviation. The sample standard deviations are compared in figure 10 with previously-acquired small-sample, "typical-area" measurements.

Figure 10 illustrates that the standard deviations increased half the time when variation was sought. From this test it is difficult to specify the population standard deviation; however, the test supports the idea that .042 (derived above) is an average minimum standard deviation, and an average population standard deviation might be a number around .07 (derived above).

Using the standard deviation, the sample size, and assuming a normal distribution of the data, an 80-percent confidence interval can be calculated. This assumption of

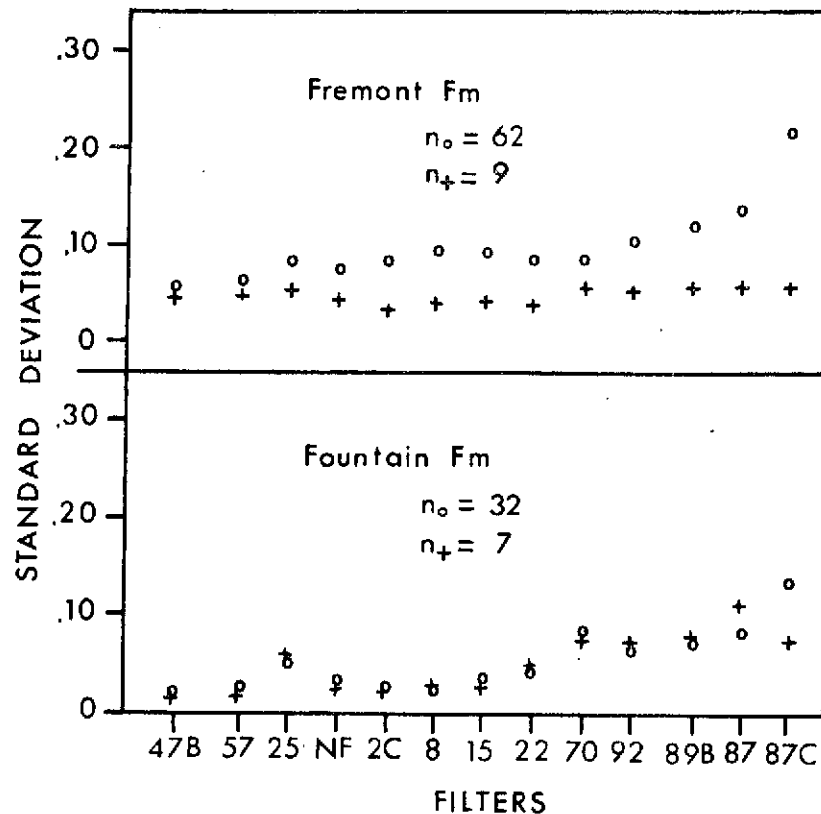
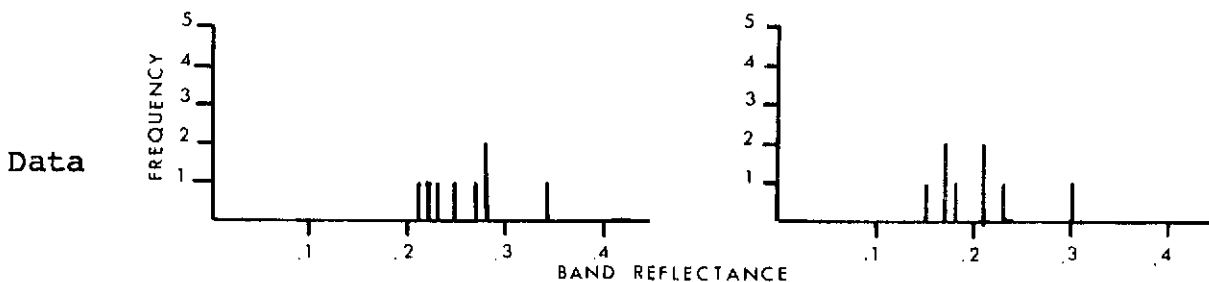


Figure 10. Sample standard deviations for the Fountain and Fremont formations. Circle (o) denotes the large sample where variation was sought; cross (+) denotes small sample measurements from "typical" outcrops. In all cases the large-sample mean band reflectance was not statistically different from the small-sample mean band reflectance. The sample sizes are denoted by n and the appropriate subscript.

a normal distribution (within each band) of the band reflectance data is justified at the 90-percent confidence level by chi-square tests of the normal distribution; see table 2 for two examples. The 80-percent confidence level was empirically selected as a level that is adequate for a data-sorting tool when comparing logarithmic plots

Table 2. Statistical summary of two typical examples of FWP band reflectance data. These data are from the lower and upper Tepee zones of the Pierre Shale with a Wratten 87C filter.

Formations Pierre Shale, Lower Tepee Pierre Shale, Upper Tepee



Number of observations	8	8
Mean	.2600	.2025
Median	.2600	.1950
Variance	.1771	.2250
Standard Deviation	.0421	.0474
Coefficient of Variation	0.16	0.23
80% confidence interval for mean	.2389 .2811	.1788 .2262
80% confidence interval for standard deviation	.0321 .0661	.0361 .0746
Chi-square test for goodness of fit to a normal distribution. Six classes used. Test statistics.	0.43	4.99
Critical Region at 10% significance level.	>6.25	>6.25
Conclusion of Chi-square test	Cannot reject that data are normally distributed so assume data are normally distributed. This conclusion is valid for most of the formations measured. It has been found empirically that this conclusion generally is made when the coefficient of variation is between .05 and .35.	

of band reflectance for different formations. For example, in those filter bands where the confidence intervals overlap, the formations are taken to have a contrast ratio of 1.0, or very close to 1.0, and are therefore not sufficiently different to be considered to have different band reflectances. See figure 11 for an example. The

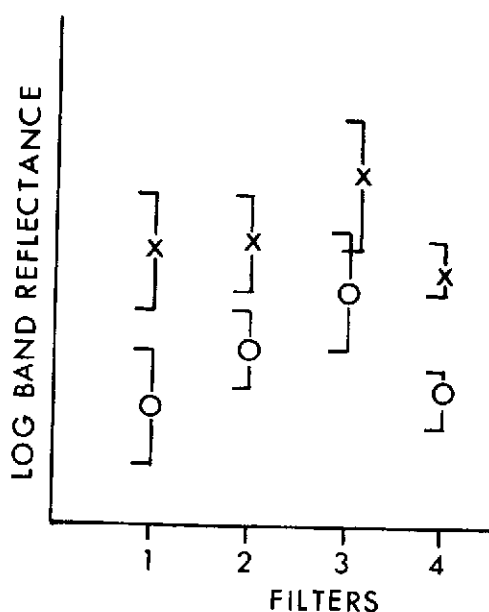


Figure 11. Use of the 80-percent confidence intervals. The x's denote the means for Formation X, the circles denote the means for Formation O, and the brackets denote the confidence intervals. Filter 1 would be considered best because of (1) no overlap of the confidence intervals and (2) maximum separation of the means (that is maximum mean contrast ratio).

validity and statistical significance of this use of confidence intervals is given by Barr (1969) and Jones and Karson (1972). Contrast ratio is the ratio of mean band reflectances, a number greater than (or equal to) 1.0.

With regard to variation between formations, figure 12 and table 3 are summaries of the contrast ratios determined

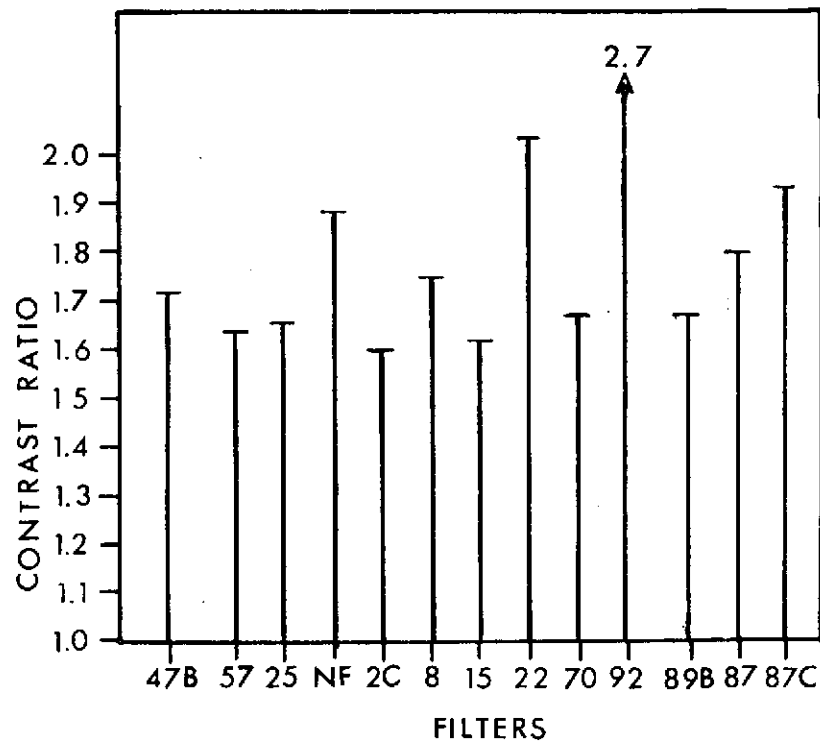


Figure 12. Range of the contrast ratios observed at the Phantom Canyon Subsite for all formations measured.

Table 3. Actual contrast ratios for the Phantom Canyon Subsite. Blanks denote a contrast ratio of 1.0.

Formations		Filters												
		47B	57	25	NF	2C	8	15	22	70	92	89B	87	87C
Pierre Shale Zones	Transition-D					1.2				1.6				1.3
	D-C	1.4	1.6		1.6	1.4	1.8		2.0	1.5	2.7	1.3	1.3	1.9
	C-Upper Tepee		1.5				1.3			1.4				
	Upper Tepee-													
	Lower Tepee-			1.7			1.2		1.6					1.2
	Lower Tepee-					1.3								
	Rusty													
	Rusty-Smoky Hills Shale	1.3		1.3			1.3	1.4	1.4	1.2	1.7	1.6	1.6	1.4
	Fountain-Fremont	1.7	2.0	1.4	1.6	1.6	1.6	1.6	1.9	1.7	1.5	1.7	1.6	1.6
	Fountain-Harding		1.4			1.2		1.2		1.4	1.2	1.3	1.2	1.3
	Fountain-Precambrian	1.4	1.4	1.3	1.2	1.3	1.3	1.3		1.4	1.4	1.5	1.4	1.4
	Fremont-Harding	1.4	1.4	1.2	1.5	1.3	1.4	1.4	1.7	1.2	1.2	1.3	1.3	1.3
	Harding-Manitou							1.2	1.2		1.2			
	Manitou-Precambrian	1.3		1.2	1.2		1.2	1.2	1.2	1.2	1.3	1.3	1.3	1.3

using mean band reflectances from the Phantom Canyon Subsite. The range of contrast ratios is very narrow, generally between 1.0 and 1.8, with very few greater than 1.8. From examination of these data, the typical difference between contrast ratios for the spectral bands considered is about 0.2. Therefore, in most cases, there are only small differences between the spectral bands considered of adjacent formations.

A statistical test of the variation, performed using analysis of variance (Koch and Link, 1970, p. 141), permits consideration of the question of whether the variation of band reflectance between formations is more significant than the variation of band reflectance within formations. Because of the large volume of data, all the data were not tested in this manner; however, units of the Pierre Shale, which are considered some of the subtlest rock discriminations made in this research, were tested. The conclusion of this test was that, in all cases, the variation between units was greater than the variation within units at the .05 significance level (95-percent confidence level). The same conclusion is therefore assumed with respect to the other formations studied.

One very important observation of all the data (shown in figure 8) is that not one single case of a statistically significant crossover in band reflectance occurred. A "significant crossover" is that case where

the mean band reflectances do cross over (relative relationship of band reflectances from one band to the next is inverse) and the confidence intervals do not overlap.

Extrapolation to Distant Areas - A question of major importance is whether these measurements made in one area (Phantom Canyon Subsite) can be used in other areas where the same formations are exposed at the surface. To answer this question, statistical comparisons were made between the same formations at the Phantom Canyon Subsite and the Gorge Hills Subsite, about 10 miles apart, and between the same formations at the Canon City Test Site and the Kassler Test Site, about 100 miles away.

The conclusion of the comparison of the Phantom Canyon data with the nearby Gorge Hills data is that the values are essentially the same. The means of band reflectance for each formation have a linear correlation coefficient of .97, and the standard deviations have a linear correlation coefficient of .67. Using a hypothesis test for equivalence of means, it was found that a systematic difference of .04 to .05 band reflectance exists between the Gorge Hills and Phantom Canyon subsites, with Gorge Hills values greater than Phantom Canyon values. This may be due to (1) slight differences in operator techniques, (2) real differences between sites, or (3) errors in data reduction. Since this difference is systematic and small, it is not considered significant.

The standard deviations do not correlate as well as the means, probably because the Gorge Hills standard deviations have a larger range and tend to be slightly larger. However, the minimum average standard deviation derived for the Phantom Canyon Subsite (.04) is a valid minimum average standard deviation for the Gorge Hills Subsite.

The conclusion of the comparison of the Kassler Test Site with the Canon City Test Site is essentially the same. The means of band reflectance for each formation have a linear correlation of about .90 and are essentially the same. This is shown in figure 13, which is a comparison of the Kassler data

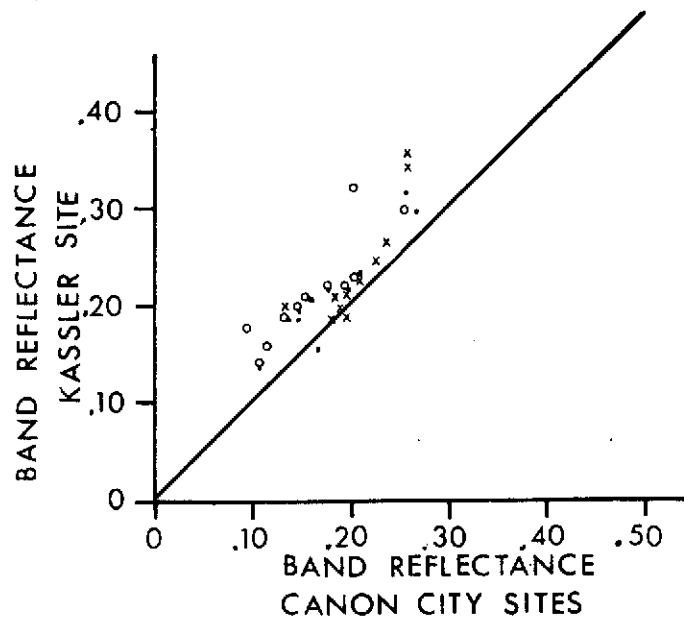


Figure 13. Comparison between band reflectance measurements from the Kassler Test Site and the Canon City Test Site. The formations considered are the upper part of the Dakota Group (o), the Fort Hays Limestone (x), and the Fountain Formation (.). The line is the line of perfect agreement. Each symbol stands for a mean band reflectance for both test sites. The Pierre Shale, as explained in Test Site Geology, is not exposed so correlations could not be made.

with the Canon City data. The average difference, where the difference is calculated as a root mean square difference, is .04 band reflectance. The standard deviations correlate very poorly; however, the .04 derived for the Canon City data is a good estimate of the minimum average standard deviation.

Therefore, it is possible to make measurements of band reflectance in one area and to use those measurements for the same formations in another area with reasonable accuracy. This assumes, of course, that the formations do not show a great deal of lateral change.

Statistical Model - It is concluded that a very simple statistical model can be used to characterize band reflectance for a formation. For any particular formation and band, the band reflectance population is normally distributed. There is significant variation of standard deviations between and within formations; however, if a minimum estimate is sufficient, the average standard deviation of the population will be about .04; however .07 is probably a better number to use. This model applies directly to those specific bands used in this research; for other bands the general conclusions would probably be about the same.

Implications of the Data - Once reflectance measurements have been made, these data theoretically can be used for the

selection of a "best" spectral band (or bands) for discriminating the measured formations by tonal contrast on aerial photography. The generally accepted technique for selection of a "best" band is to select that band having the maximum contrast ratio for the formations being considered (where the contrast ratio is defined as the ratio of the band reflectance of the two formations being considered, and, by convention, a number greater than or equal to 1.0). The reason for using the contrast ratio is that it is a mathematical relationship that relates the resulting film density to the exposure of the film.

In order to select the band with the maximum contrast ratio, it is necessary to question if this ratio is larger than the contrast ratios of all other bands. Using the data from the previous sections, this question can be answered in the following manner. However, it should be remembered that a statistically-significant difference in contrast ratio is not necessarily visually detectable on aerial photography.

As depicted in figure 14, a minimum-maximum interval (min-max interval) for the mean contrast ratio can be derived that is similar to, and derived from, the 80-percent confidence intervals for the band reflectance means of each band for two adjacent formations. Then, using this min-max interval for the contrast ratio, the equations for the 80-percent confidence interval for the band reflectance mean,

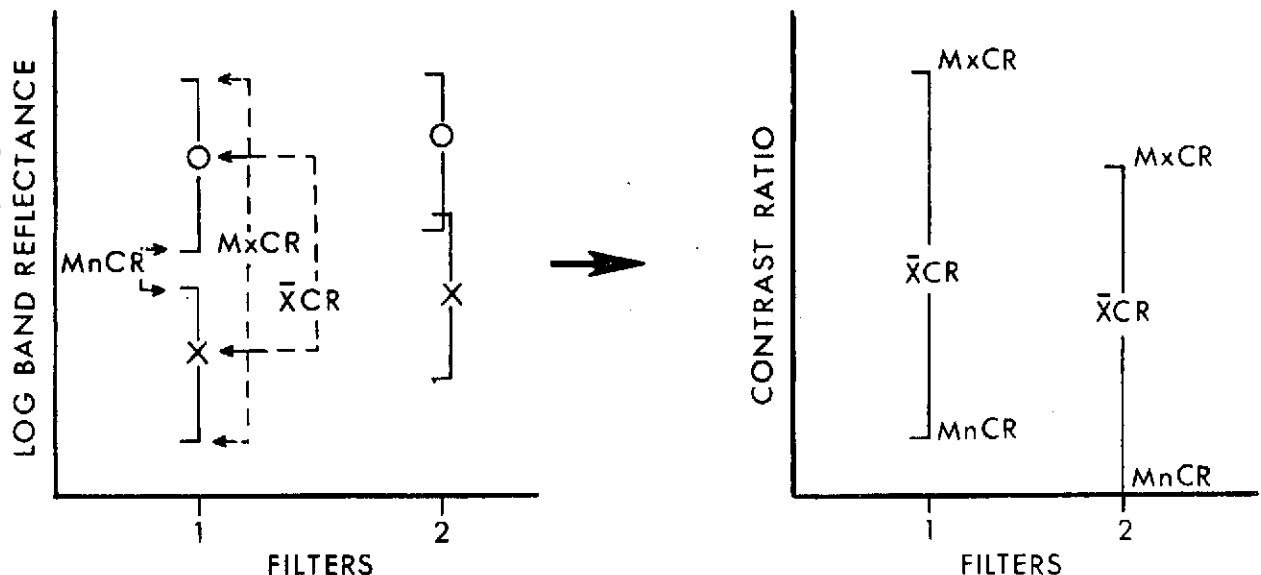


Figure 14. Definition of the min-max interval on the contrast ratio. The log band reflectance plot is used for comparison of Formations X and O because with this plot the contrast ratio plot with min-max intervals can be visualized. It can be seen that the min-max intervals for filters 1 and 2 would overlap in the example given. Calculation of the min-max interval would be as follows: for the minimum value of the interval, ratio the antilog of the numbers marked by the MnCR arrow; for the maximum value, ratio the antilogs of the numbers marked by the MxCR arrows, and for the mean contrast ratio, ratio the antilogs of the numbers marked by the $\bar{X}CR$ arrows. This min-max interval is used like a confidence interval.

and the data summarized in Data Summary, the number of measurements per band per formation (sample size) required to be statistically confident that the contrast ratios are different (non-overlapping min-max intervals) can be calculated. Because of the lack of established statistical procedures for this type of calculation, the derived sample sizes can be treated only as order-of-magnitude figures.

An example of the calculation procedure is given in table 4 and the results in table 5.

Table 4: Actual example of the calculation procedure used to determine the minimum sample size. The data used are from table 2.

$\bar{w} \pm \frac{t \cdot s}{\sqrt{n}}$	Student's confidence interval t = Student's statistic, s = sample standard deviation n = sample size \bar{w} = sample mean
$\frac{.2600}{.2025} = 1.25$	Mean contrast ratio in a given band for two adjacent formations with mean band reflectances of .2600 and .2025 respectively
$\frac{.2525}{.2100} = 1.20$	Minimum contrast ratio
$\frac{.2675}{.1950} = 1.37$	Maximum contrast ratio
	$\pm .0075$ interval on the mean band reflectance and approximately a $\pm .08$ interval on the contrast ratio
$\frac{t \cdot s}{\sqrt{n}} = .0075$	From confidence interval and assuming t = 1.3 and s = .043
n = 53.7	Sample size = 54

Table 5. Relationship between sample size (n), sample standard deviation (s), the differences between mean contrast ratios (D), and the length of the interval on the contrast ratio (LCR). These sample sizes are justified as order-of-magnitude estimates only.

s	.02	.038	.042	.070	.10	D	LCR
n	28	100	121	332	676	.10	$\pm .05$
	12	45	54	147	300	.16	$\pm .08$
	7	25	31	82	169	.22	$\pm .11$
	2	7	8	21	42	.44	$\pm .22$

Thus from table 5 and the generalizations that the minimum average standard deviation is .042, that an average population standard deviation is about .07, and that a typical difference between mean contrast ratios is approximately .16

(see table 3), it is evident that the number of measurements required in order to select the "best" band for the discrimination of two formations is between 150 and 300 measurements per filter per formation. I consider this number of measurements too large for a practical technique.

As a further test of this conclusion and as a suggested procedure for future research, the following observation is offered. If a confidence level of 95 percent for the band reflectance mean had been used instead of an 80-percent confidence interval, then in almost all cases the confidence intervals on a log band reflectance - filter plot (such as figure 11) would have overlapped. Thus, the same type of conclusion concerning sample size would have been drawn more easily and rapidly. This observation, of course, is derived in retrospect and applies to these data only.

Further support of the conclusion that a "best" band or set of bands cannot be practically selected can be gained by analysis of the relative amplitude variation of band reflectance between formations. Figure 15 was prepared by normalizing the grand mean band reflectance data so that the NF band has a value of 1.00. The circles are the normalized grand mean of all formations and the dashed lines are the normalized 80-percent confidence interval. The circles and confidence intervals are connected between bands for visualization. Then, normalizing the mean data

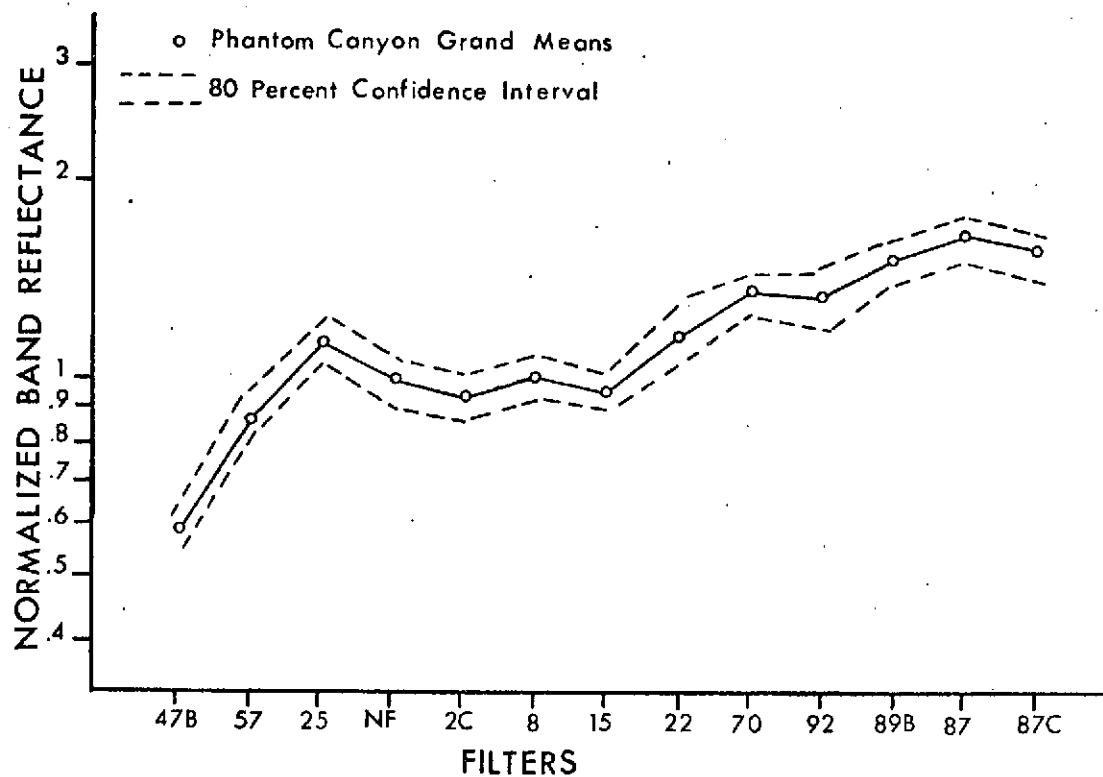


Figure 15. Normalized band reflectance. "Normalized" means all means were divided by the NF mean band reflectance. The NF band was selected because the NF band averages over the full spectrum. All observed mean band reflectances are not different from the means shown in this graph at 95-percent confidence.

for each formation, it was found statistically that each of the means did not differ from the normalized grand mean at the 95-percent confidence level. Therefore, the differences between the band reflectance data for most formations have a constant relative difference that is independent of wavelength.

If this conclusion is valid, then by using one known band reflectance, the band reflectance for the other 12 bands

can be calculated. An empirical solution of this prediction takes the form:

$$B_i = B_m \times P_i$$

where

B_i = an unknown band reflectance, $i=1, \dots, 12$

B_m = the known or measured band reflectance

P_i = the proportionality factor between B_m and B_i ,
 $i=1, \dots, 12$.

Selecting the NF band as the known band reflectance, because this band averages across the full spectrum, and using the grand mean data from the Phantom Canyon Subsite to derive P_i , the results in table 6 were derived. The average error is a root mean square error. From inspection of table 6, it can be seen that the error is generally less than the minimum average standard deviation, .04 band reflectance.

Discussion

In the Data Summary, I have summarized the rock band reflectance properties of more than 8,600 measurements from the Canon City and Kassler test sites, shown that for any spectral band the data are normally distributed and simple statistics can be used, and most significantly, determined that an impractically large number of observations (150 to 300 per band per formation) is required in order to

Phantom Canyon

Filter	Grand Mean Band Reflectance	Precambrian		Manitou Fm.		Fremont Fm.		Fountain Fm.		Rusty zone		Lower Tepee zone		C Unit		Average Row Error	
		P	M	M	C	M	C	M	C	M	C	M	C	M	C		
NF	.166		.144		.120		.198		.122		.176		.181		.113		
47B	.099	0.596	.093	.086	.071	.072	.112	.118	.065	.073	.100	.105	.097	.108	.073	.067	.007
57	.147	0.886	.117	.126	.101	.106	.168	.175	.082	.108	.189	.156	.139	.160	.113	.100	.020
25	.192	1.157	.181	.167	.150	.139	.203	.229	.144	.141	.206	.204	.235	.209	.175	.131	.025
2C	.157	0.946	.136	.136	.124	.114	.173	.178	.108	.115	.204	.166	.154	.171	.117	.107	.019
8	.168	1.012	.149	.146	.120	.121	.185	.200	.118	.123	.183	.178	.180	.183	.112	.114	.007
15	.160	0.964	.145	.139	.120	.116	.189	.191	.116	.118	.160	.170	.157	.174	.145	.109	.017
22	.194	1.169	.143	.168	.125	.140	.249	.231	.130	.143	.215	.206	.212	.212	.141	.132	.016
70	.227	1.367	.205	.197	.174	.164	.243	.271	.145	.167	.270	.241	.227	.247	.174	.154	.023
92	.222	1.337	.211	.193	.163	.160	.241	.265	.157	.163	.211	.235	.212	.242	.132	.151	.021
89B	.253	1.524	.252	.219	.193	.183	.283	.302	.169	.186	.230	.268	.251	.276	.235	.172	.036
87	.273	1.645	.261	.237	.203	.197	.297	.326	.183	.201	.259	.290	.334	.298	.239	.186	.034
87C	.258	1.554	.268	.224	.205	.186	.297	.308	.187	.190	.259	.274	.260	.281	.189	.176	.023
Average Column Error			.021		.010		.019		.014		.025		.022		.032		

Gorge Hills-Florence SE

Kassler

Filter	Fremont Fm.		Fountain Fm.		B Unit		D Unit		Fountain Fm.		Lyons Sandstone		Glennon Limestone	
	M	C	M	C	M	C	M	C	M	C	M	C	M	C
NF	.265		.112		.172		.137		.146		.237		.329	
47B	.138	.158	.081	.067	.117	.103	.113	.082	.101	.087	.148	.141	.232	.196
57	.210	.235	.096	.099	.171	.152	.148	.121	.109	.129	.194	.210	.319	.291
25	.298	.307	.169	.130	.209	.199	.192	.159	.184	.169	.256	.274	.357	.381
2C	.233	.251	.103	.106	.156	.163	.135	.130	.118	.138	.220	.224	.330	.311
8	.253	.268	.103	.113	.147	.174	.127	.139	.119	.148	.246	.240	.235	.333
15	.293	.255	.119	.108	.159	.166	.130	.132	.118	.141	.239	.228	.338	.317
22	.282	.310	.151	.131	.183	.201	.171	.160	.151	.171	.237	.277	.356	.385
70	.202	.362	.215	.153	.207	.235	.210	.187	.315	.200	.295	.324	.373	.450
92	.299	.354	.189	.150	.199	.230	.203	.183	.247	.195	.259	.317	.357	.440
89B	.403	.404	.243	.171	.233	.262	.226	.209	.272	.223	.336	.361	.460	.501
87	.384	.436	.243	.184	.216	.283	.231	.226	.289	.240	.346	.390	.450	.541
87C	.383	.412	.253	.174			.284	.213			.394	.368	.395	.512
Average Column Error	.057		.045		.030		.029		.050		.030		.060	

Table 6. Calculated band reflectance. Average error for all the Phantom Canyon data is .021. Grand average error of all data shown is .035. Average error is a root-mean square type error. P is the proportionality factor between the measured values and the NF band reflectance. M is the measured value and C is the calculated value.

select best filters. With this foundation, I will discuss what this statistical analysis means with regard to rock discrimination by multiband photography.

Concerning the general applicability of the conclusions drawn, the formations considered have not been selected in a statistical manner that would allow statistical inferences to be made about all rocks, or even all sedimentary rocks. However, there is no geologic reason to suspect that the rocks and formations considered have unique reflectance properties with regard to other sedimentary rocks. Therefore, the conclusions drawn apply in detail only to the formations considered; however, generalizations of conclusions are probably valid for most sedimentary rocks.

The conclusion to be drawn from the previous section is that there is no practical numerical basis for selecting any particular spectral band as best for rock discrimination and, in most cases, there is little numerical basis for selecting better spectral bands. Therefore, useful information for the design of multiband photography cannot be obtained from the band reflectance data considered here. As an example to clarify this statement, consider a comparison between the Munsell-color-cards example shown in figure 1 and the rock reflectance problem considered in this dissertation. The Munsell color cards are manufactured under very controlled conditions; therefore, their reflectance

is very uniform. If numerous, repetitive measurements of the reflectance of these cards were made with a very precise instrument, a standard deviation near zero would be obtained and, therefore, a confidence interval on the mean would have a length of approximately zero. That is, with almost complete confidence, the band reflectance differences tabulated in table 1 are as shown, and valid tonal contrast between the Munsell cards could be predicted with this band reflectance information so best bands could be selected. However, in situ-measured rock band reflectance is so variable that it is not possible to predict tonal contrast between formations precisely enough to define which are the best spectral bands or in most cases, even better spectral bands.

The problem is further complicated because (1) many smaller shrubs and topographic effects cannot be resolved on aerial photography and (2) the atmosphere and atmospheric effects can be significantly variable. Thus, the variation that is encountered on aerial photography is even larger than that of rock band reflectance alone. Therefore the multiband photography concept as shown in figure 1 does not have a practical numerical basis from which the concept can be applied to rock discrimination. This implies that the information content of all spectral bands, or combinations of bands, should be the same.

Finally, the 13 mean band reflectances can be calculated by knowing one of those means. Therefore, similar differences of band reflectance exist between all the spectral bands for any two formations. Thus, there is no best band or bands for sedimentary rock discrimination where residual soils and rocks are observed.

Filter Selection

Although the numerical analysis in the previous section indicates that there is no "best" filter or filters to discriminate the formations at the Phantom Canyon Subsite, it was decided to select the best estimate of the "best" film/filter combination and to subjectively test this "best" photography in order to test the numerical conclusion. The criteria used to select the best estimate of the "best" band for discrimination of a formation contact is: that band is "best" that has no overlap of the confidence intervals of the two formations being considered and that has the maximum mean contrast ratio (i.e. maximum ratio of sample mean band reflectance). Then the "best" combination of bands is selected that will discriminate the largest number of formations with maximum redundancy. Operationally, this definition of "best" is used by visually inspecting overlaid log band reflectance plots (see Appendix A) and compiling a matrix like Table 7. The number of bands selected and the film type are further restricted by the camera to be used. In this case a multiband camera that uses only one film type at a time was used.

The selection matrix for the Phantom Canyon data from which to select the four "best" bands is tabulated in table 7.

Table 7. Phantom Canyon selection matrix. "Good" filters are marked G and "best" filters are marked B. More than one "best" in a row means that any difference between those filters is insignificant. "Best" means no overlap of the 80-percent confidence interval and maximum separation of the mean of median. "Good" means no overlap of the 80-percent confidence interval. See table 8 for the selected filters.

Lithologic Units	Filters												
	47B	57	25	NF	2C	8	15	22	70	92	89B	87	87C
Upper Transition-D					G					B			G
D-C	G	G		G	G	G		G	G	B	G	G	G
C-Upper Tepee		G				G			B				
Upper Tepee-Lower Tepee			G			G		B					G
Lower Tepee-Rusty					B								
Rusty-Smoky Hill	G		G			G	G	G	G	B	G	G	G
Fountain-Harding		B			G		G		B	G	G	G	G
Fountain-Fremont	G	B	G	G	G	G	G	G	G	G	G	G	G
Fountain-Precambrian	B	G	G	G	G	G	G		G	B	G	G	G
Fremont-Harding	B	B	G	G	G	G	G	G	G	G	G	G	G
Harding-Manitou							G	G		B			
Manitou-Precambrian	G		G			G	G	G	G	B	G	G	G
Quaternary gravel-Smoky Hill								B	G		G		
Quaternary gravel-Rusty		G	G	G	G	G		G	B			G	G
Quaternary gravel-Lower Tepee		G	B	G		G		G	G	G	G	G	G
Number of "Bests"	2	3	1	0	1	0	0	2	3	5	1	0	0

The selection matrix for the Phantom Canyon data from which to select the four "best" bands is tabulated in table 7. In addition, those filters with no overlap of the 80-percent confidence intervals (i. e., "good" discrimination) are noted. As discussed in the Data Summary section, these "good" filters are statistically neither worse nor better than those called "best". The "best" bands and the formations that each will discriminate are tabulated in table 8.

Table 8: The "best" filters and the formations discriminated "best". See plate 1 for definition of symbols.

"Best" Bands	Formations Discriminated "Best"
92	Kpt-Kpd, Kpd-Kpc, Kpr-Ks, Oh-Om, Om-pe
57	Pf-Oh, Pf-Of, Of-Oh
70	Kpc-Kpuf, Pf-Oh, Qg-Kpr
22	Kplt-Kput, Qg-Ks

Using the above criteria for generating a selection matrix, with the added criterion that the range of the band reflectance measurements was inspected and the redundancy criterion was not used, another selection matrix was developed for the Gorge Hills and Florence SE Subsites as shown in table 9 and the four "best" filters are those in table 12 (p. 62).

Table 9. Gorge Hills-Florence SE subsites selection matrix. The symbols are defined at the bottom of the table.

Formations	Filters												
	47B	57	25	NF	2C	8	15	22	70	92	89B	87	87C
Upper Transition-CD	Q	G	G	G	G	F	F	G	N	F	G	G	N
CD-Upper Tepee	Q	G	G	G	G	G	G	G	N	F	G	Q	N
Upper Tepee-Lower Tepee	Q	P	P	P	P	P	P	P	N	Q	P	P	P
Lower Tepee-Rusty C	N	N	N	N	N	N	Q	N	N	N	N	N	N
Rusty C-Rusty B	N	N	N	Q	Q	N	Q	N	N	N	N	Q	N
Ft Hays - Carlisle	P	N	P	P	P	P	P	P	P	P	P	P	P
Carlisle-Greenhorn	F	Q	P	P	P	Q	P	Q	P	Q	P	P	Q
Greenhorn-Graneros	F	P	F	P	P	P	F	P	F	F	F	F	F
Graneros-Dakota	P	F	F	F	F	F	F	F	F	F	F	F	F
Dakota-Purgatoire	G	G	G	G	G	G	G	G	F	F	F	F	F
Purgatoire-red Morrison	N	N	F	N	P	F	F	F	Q	F	F	P	P
red Morrison-green Morrison	P	F	G	G	G	G	G	G	Q	F	F	P	Q
green Morrison-Entrada	Q	P	P	P	P	P	P	P	N	N	N	N	N
Entrada-Fountain	G	G	Q	G	F	P	F	P	N	N	N	N	N
Fountain-Fremont	P	F	F	F	F	F	F	F	N	F	F	F	Q
Fremont-Harding	N	P	N	N	P	P	P	P	Q	Q	N	N	N
Harding-Precambrian	P	P	P	P	P	P	P	P	P	P	P	G	P
Ranking	8	2	6	1	2	4	4	6	12	11	9	10	13

Symbols	Mean,Median	Confidence intervals	Distribution of raw data
G Good	wide separation	wide separation	all separate
F Fair	wide separation	separation	all separate
P Poor	separation	separation	overlap
Q Questionable	separation	some overlap	overlap
N No Good	little separation	large overlap	overlap

The differences between these two sets of "best" filters can be explained by differences in selection criteria, subtle differences in the basic reflectance data that may be related to the number of samples necessary for selection of "best" bands, and differences in geologic expression (see pls. 1 and 2). The diagrammatic geologic cross sections shown on figure 16 show an example of the significance of geologic expression.

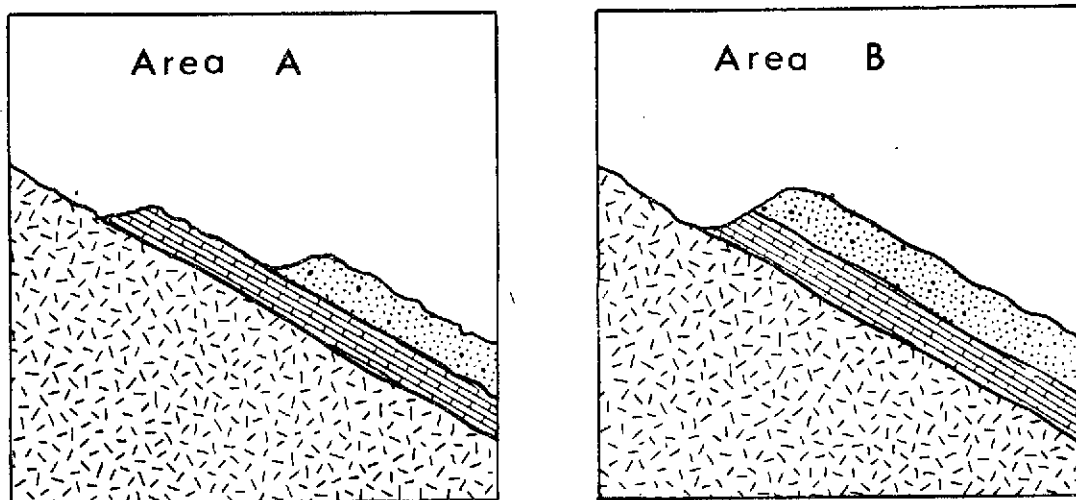


Figure 16. Effect of geologic expression upon selection of best filters. In Area A, all three formations are important, whereas in Area B, the limestone formation, which is exposed in a near-vertical cliff, may be practically unobservable on aerial photography. The more practical discrimination in Area B would be between the sandstone and igneous formations.

Thus, for the selection of best filters, it is necessary to consider the geologic exposure and the importance of distinguishing or combining particular formations for the

problem to be solved.

With regard to film selection, there are two major considerations: spectral sensitivity and effective film speed. These two considerations eliminate most films from consideration because there is only one usable film with sensitivity to the photographic infrared (Kodak Infrared Aerographic Film Type 2424) and there is little spectral sensitivity difference between the usable films that are sensitive to visible light (400 to 700nm). Therefore, there are no decisions to be made; the filters selected define which film can be used.

AERIAL MULTIBAND PHOTOGRAPHY

After having selected a set of "best" filters and decided upon a film, it is necessary to acquire the multi-band photography. This section discusses the acquisition of the multiband photography used in this research.

All aerial photography was acquired under subcontract by Mr. Robert Hardwick of Hardwick and Associates, Arvada, Colorado, using an International Imaging Systems (I²S) multi-band camera. This camera produces four simultaneous 3.5- by 3.5-inch photographs in a single frame in four spectral bands using a single roll of 9-inch film. Kodak Infrared Aero-graphic Film Type 2424 (a negative black and white infrared film) was used. Details of the camera system are described by Ross (1973). The photography was flown generally at a 1:12,000 scale along north-south flight lines, within three hours of solar noon in the months of August and September, 1972 and 1973. Atmospheric conditions at the time of photo flights were generally excellent. The film was processed by Mead Technology Laboratories, Dayton, Ohio, to I²S specifications (1971 specifications, Wratten 88A band processed to a gamma of 1.9), and positive transparencies were processed at a copy gamma of 1.0.

To determine the correct exposure, test photography was flown with all filters. The correct exposures for each

filter were determined by inspection of these tests (table 10). Even with this testing, changes in the atmosphere and/or camera malfunctions resulted in having to re-fly a few sets of filters in order to obtain good exposures. Thus, correct exposure is a very real problem when using multiband photography.

Table 10. Best exposures for the filters considered. Determined from test aerial photography over the Canon City Test Site in August and September near 1200 hours. For Kodak Infrared Aerographic Film Type 2424. IRB means infrared blocking filter. All of the filters are Wratten gelatin filters, except NF as noted previously.

Filter	f-stop	Speed (secs)
47B + IRB	4.5	1/250
57 + IRB	3.5	1/250
25 + IRB	3.5	1/250
NF + IRB	13.5	1/250
2C + IRB	9.5	1/250
8 + IRB	8	1/250
15 + IRB	6.8	1/250
12 + IRB	5.6	1/250
22 + IRB	6.8	1/250
70 + IRB	8	1/250
92 + IRB	4.5	1/250
89B	16	1/250
87	11	1/250
87C	8	1/250

In order to give a potential user of multiband photography an idea of the cost of acquiring multiband photography,

the costs are summarized in table 11. It should be recognized that the test sites were all local, therefore the costs include only the actual data acquisition and processing costs.

Table 11. Cost of acquiring multiband photography (December, 1973).

Item	Cost
1. Rental of I ² S camera and intervalometer, including shipping from Mt. View, California, to Denver, Colorado.	\$850/month
2. Film, Kodak Infrared Aerographic Film Type 2424 (250 ft).	\$120
3. Aerial photographer, pilot, and plane (twin-engine Apache)	
Fuel.	\$30/hour
Plane, pilot, and photographer.	\$120/hour
Crew mobilization charge.	\$120/day
4. Film processing.	
Negative and positive transparencies	\$315
Sensitometry, relative exposure	\$10/filter
Shipping (Denver, Colo., to Dayton, Ohio).	\$26
Minimum cost for a one-day job (approximately 5 hours flying) and one roll of film. Assumes exposures known and no transit costs.	\$2221

PHOTOGRAPHIC DATA ANALYSIS

The objective of the research reported in this dissertation was to evaluate multiband photography for rock discrimination. Therefore, even though the numerical analysis indicates that the essential first step of designing a "best" multiband configurations cannot be made, it is necessary (1) to test this conclusion, (2) to answer questions concerning the significance of differences in contrast ratios, and (3) to determine if some other filter-selection procedure might allow users to use multiband photography successfully. The reason that these questions have to be answered from the analysis of aerial photography is that the numerical analysis tested only for numerical differences and not necessarily for differences that would be visible to a human interpreter. Therefore, the conclusions need to be tested under actual working conditions with aerial photography. This discussion will consist of two parts, (1) a discussion of the aerial multiband photography and of the methods of using this photography and (2) a non-numerical evaluation of the results. The word non-numerical is used here to contrast this analysis of the aerial photography with the objective numerical analysis and to emphasize that the analysis presented is my own evaluation. Numerous examples of the photographs evaluated are presented in plates 3 through 7 in order

to support the analysis presented. Table 12 is a tabulation of the multiband combinations tested. The term combination is used to mean a filter (or filters) used with a particular film.

Table 12. Combinations of filters evaluated. Details for each combination are given in the text. See figure 5 for the passbands of these filters. The meaning of "Displays Produced" is discussed in the text (p.65).

Combination Name	Films and Filters Used	Displays Produced or Uses
1. Standard Black and White	Panchromatic 12 or 15	Black and white, MAC ¹
2. Standard Multiband	Black and White IR 47B, 57, 25, and 88A	Color, CIR ² , MAC
3. Phantom Canyon Design	Black and White IR 57, 22, 92, and 70	MAC
4. Gorge Hills-Florence SE Design	Black and White IR 47B, 8, 25, and 87	MAC
5. Contrast Ratio Test	Black and White IR 8, 15, 70 and 92	To test the significance of predicted contrast-ratio difference

Before beginning the discussion of the aerial photography, it is beneficial to discuss the concept of color additive viewing, the color additive viewer (CAV), and the specialized terminology that is used. The concept of color

¹MAC display is an abbreviation for a manipulated additive color display and does not include color and CIR displays.

²CIR is an abbreviation for color infrared.

additive viewing was demonstrated by Maxwell in 1861 (Smith and Anson, 1968). The concept is that all colors can be produced by adding together certain amounts of the three "additive primary colors". The "additive primary" colors are those colors that cannot be made from other colors; the "additive primary colors" are blue (Wratten 47B), green (Wratten 57), and red (Wratten 25). Operationally, this concept is made use of in CAV which is shown diagrammatically in figure 17. If, for example, the Standard Multiband

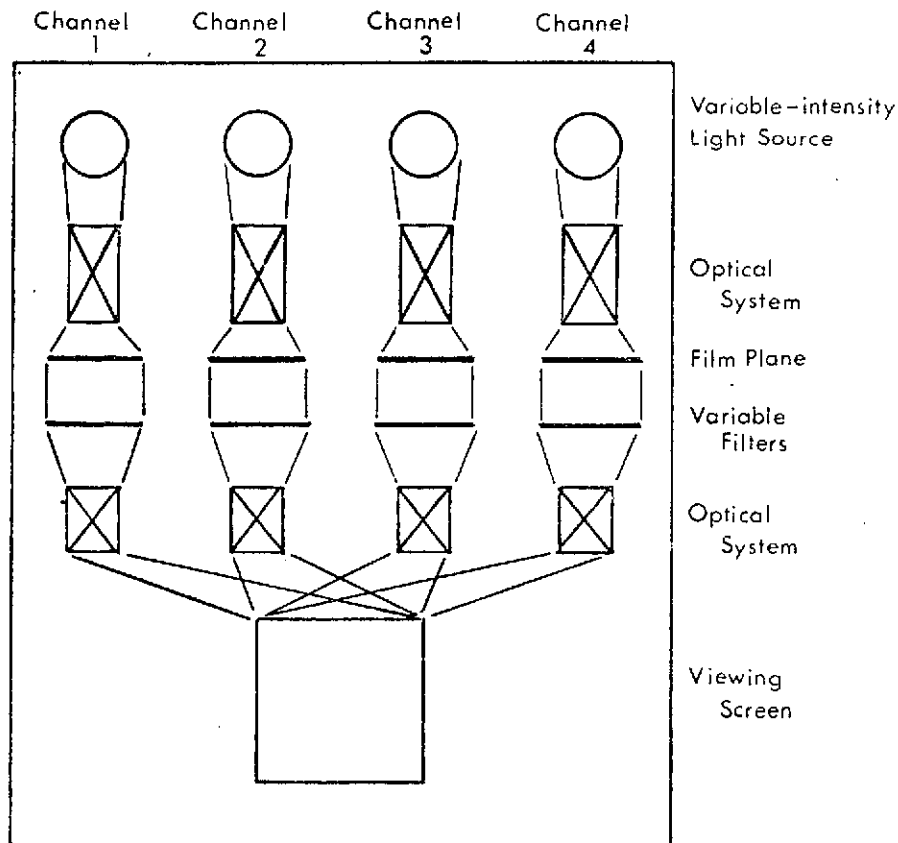


Figure 17. Diagram of the color additive viewer.

Combination is placed in the film plane the following operation can produce an image that has colors like those of the area photographed. The following filters are inserted in the optical path with the associated photographed band, blue - 47B, green - 57, and red - 25. Then, by adjusting the light intensity of each channel, which is modulated by the film, a color display results by addition of colors. The 47B photograph is said to be coded blue, the 57 is coded green, and the 25 is coded red. The resulting image is referred to as a "display", specifically a "color display" in this example. As another example, to produce a display like that obtained with color infrared film (CIR film), the 57 is coded blue, the 25 is coded green, the 88A is coded red, and the light intensities are appropriately adjusted. This last example is called a "CIR display". Any channel that is not used has the light source turned off. The appropriate adjustment of the light is judged by eye and is a function of CAV filter density, film exposure, film processing, variables of the atmosphere and the area photographed, and human color perception. Therefore, the evaluations of the color additive displays are non-numerical evaluations based upon numerous physio-psychological factors (Ross, 1973). The theory of the use of a CAV is discussed by Yost and Wenderoth (1967) and Ross (1973).

CAV Displays

There are three classes of film/filter combinations and several viewing methods that were considered during this research. The three classes are (1) the Standard Multiband Combination, (2) the Standard Black and White Combination and (3) the Designed Combinations, defined in table 12. Aerial multiband photography using the I²S camera of all three of these combinations and those filters not selected for a particular combination was acquired of the Canon City Test Site, and all the designed combinations were acquired of the Kassler Test Site. The viewing methods are the various types of displays that can be produced from a film/filter combinations.

The Standard Multiband Combination, referred to as Standard MB Combination, is a division of the photographic region of the electromagnetic spectrum into four divisions. These four divisions are defined by the Wratten filters 47B, 57, 25, and 89B (figure 5, pg 25) with black and white infrared film, and are the same spectral bands used in color and CIR films. The displays that can be produced with this combination are color, CIR, and MAC displays. Plate 3 shows photographs of color and CIR displays, and plates 5 (A and E) and 6 (A, C, E, and G) are prints from the Standard MB Combination. MAC displays are discussed later. The advantages and disadvantages of using the

Standard MB Combination, and multiband photography in general, in comparison with color and CIR photography, are listed in table 13.

Table 13. Inherent advantages and disadvantages of the Standard MB Combination in comparison with color and color infrared photography.

Advantages

1. Black and white film is cheaper, and processing is cheaper and easier.
2. Subtle color-balance changes on color and CIR displays can be easily made, frame by frame, in real time.
3. Spectral information is more readily available.

Disadvantages

1. Photographers have less experience with multiband photography.
2. Exposure problems are more critical because four simultaneous exposures are being made that must be properly balanced.
3. In order to get stereo-pairs or any hard copy of the display, the display has to be photographed, resulting in image and tonal degradation.
4. Four photographs are being used instead of one so interpretation time increases.
5. No best systematic way is known to work with these four photographs.

The second combination class to be considered is the standard black and white aerial photography referred to as Standard B/W Combination. This photography uses the visible part of the electromagnetic spectrum minus the atmosphere-affected blue spectral band. This band is defined by the

Wratten filters 12 or 15 (figure 5, p. 25) with panchromatic film. The quality of this type of photography, as acquired in print forms from several government agencies, is normally greatly reduced because of dodging and the use of paper prints. The quality of this type of photography can be greatly increased and properly compared with other combination classes by using non-dodged, original transparencies. For these reasons, this combination was acquired with the I²S camera using both the Wratten 12 and 15 with Kodak Plus-X Aerographic Film 2402. Examples can be seen in plate 5 (A and B). MAC displays can be made with this combination class also. Table 14 lists the inherent advantages and disadvantages of this combination in comparison with the Standard MB Combination.

The third combination class consists of the designed combinations which can consist of any group of filters and films that the user desires. The specific combinations considered here are numbers 3, 4, and 5 in table 12. Plates 4 (C, D, E, and F), 5, and 6 are prints from these configurations. MAC displays can be made with this combination class also. Table 15 lists the inherent advantages and disadvantages of this combination class in comparison with the Standard MB Combination.

Table 14. Inherent advantages and disadvantages of the Standard B/W Combination in comparison with the Standard MB Combination.

Advantages

1. Photographers have long experience with the Standard B/W combination.
2. There is no redundancy of information because only a single photograph is being interpreted.
3. Interpreters have many years of experience to draw upon.
4. Years of use have shown that useful information can be obtained.
5. Photography has already been acquired of many areas of the world.

Disadvantages

1. Spectral information is not available.
2. Color and CIR displays cannot be produced.

Table 15. Inherent advantages and disadvantages of the designed combinations in comparison with the Standard MB Combination.

Advantages

1. Selected spectral information is available.
2. If a set of best bands exists and can be defined, this information can be used.

Disadvantages

1. Photographers have little or no experience with many of the filters used.
2. The I²S camera must be modified to assure that the photographs will register. This modification is now a standard option available for the I²S camera.
3. Extensive knowledge of the area to be photographed is required in order to design the combination.
4. No procedure is known for producing displays from this combination that can be intuitively interpreted.

The rationale for designing the Phantom Canyon and the Gorge Hills-Florence SE designed combination is given in the Filter Selection section. The rationale for designing the Contrast Ratio Test Combination (table 12) was to test predicted contrast relationships, that is the significance of the observed contrast ratio differences between the filters considered. Table 16 summarizes the data used to design the Contrast Ratio Test Combination and the predicted aerial photography contrast relationships for the Fountain and Lyons formations at the Kassler Test Site. See plate 4 (C-F) for examples of the resultant photography. Using the numerical analysis procedure (described in the Data Summary section), the 8 and 15 filters are statistically better than the 70 and 92 filters; however it is not statistically possible to say which of the 8 or 15 is best nor which of the 70 or 92 is worse.

Table 16. Reflectance data and predictions concerning contrast of the Fountain and Lyons formations. Data are from the Kassler site and include 12 and 16 measurements, respectively.

Filter	Mean Band Reflectance		Contrast Ratio			Predicted Contrast
	Fountain Fm.	Lyons Fm.	Mean	Min.	Max.	
	8	11.9	24.6	2.06	1.72	
15	11.8	23.8	2.02	1.75	2.31	Good
92	24.7	25.9	1.05	1.00	1.47	Poor
70	31.5	29.5	1.07	1.00	1.13	Poor

The viewing procedures for color and CIR displays have already been described. The final procedure, the manipulated additive color displays (MAC displays), requires description. Several examples of MAC displays are shown in plate 3 (D-F) and plate 7. The term MAC display is used for any color-coded display other than color and CIR displays. Table 17 summarizes the definitions of color, CIR, and MAC displays.

Table 17. Definition of color, CIR, and MAC displays.

<u>Display Name</u>	<u>Filter-Coding</u>
Color Display	47B - blue, 57 - green, 25 - red
CIR Display	57 - blue, 25 - green, 88A - red
MAC Display	Any other coding method, including photographic manipulation of the original photography before coding.

The most successful technique for producing MAC displays is to make high-contrast copies at different exposures of the original film (positives and negatives), and then to recombine selected positive- and negative-high-contrast copies in register with coding to produce the MAC display. Details of the procedure are given in Appendix B. The MAC displays in plate 7 were produced using this procedure. This technique, as discussed later, is considered the most successful, because, with this technique, maximum tonal (black and white and color) discrimination of the formations was obtained.

The rationale for developing this high-contrast, positive-negative technique was derived from the numerical analysis. The primary factors considered are (1) the lack of cross-overs in the band reflectance data and (2) the low contrast in the contrast ratios. The high-contrast film increases the photographic contrast between rocks, and the use of positives and negatives simulates cross-overs. These two operations are equivalent to the numerical signal stretching and ratioing techniques that seem to be very useful procedures for enhancement of numerical remote sensing data, such as ERTS imagery (Kenneth Watson, 1973, personal communication).

Finally, those bands not selected for any configuration, NF, 2C, and 87C, were also acquired. Thus, individual bands can be compared to test if one of these might be better than predicted. From visual inspection and comparisons, these bands were better than predicted because all formations can be discriminated as easily as with those bands predicted to be better. A visual evaluation of most bands can be made by comparing plates 3 through 6.

Evaluation of Aerial Multiband Photography

From the previous section it is obvious that numerous viewing methods can be used with multiband photography. A subjective analysis of the Contrast Ratio Test Combination and the high-contrast, positive-negative MAC displays will be

discussed. The conclusions to be presented are (1) that the differences in contrast ratios between all the filters considered are not significant and (2) that the spectral information in different bands is not advantageous.

Plate 4 (C-F) shows aerial photography obtained with the Contrast Ratio Test Designed Combination. It was predicted (see table 16, p. 69) that the 8 and 15 bands should be better than the 70 and 92 bands. From visual evaluation of the original photography and from video-density-slicing techniques, it is concluded that there are not significant improvements in contrast differences between the Fountain and Lyons formations in these four spectral bands. Therefore, even for differences in contrast ratios as large as 1.0 (from table 16), improvement in contrast does not result. Thus, the typical difference in contrast ratio of 0.2 is not a significant difference for human photogeologic interpretation, and a difference of contrast ratios larger than 1.0 is probably necessary for significant improvement.

In the process of working with the high-contrast, positive-negative MAC technique, it was found that it was not necessary to use different spectral bands in order to produce excellent rock discrimination. Excellent rock discrimination can be produced by the high-contrast, positive-negative masking technique using MAC displays from only one spectral band (see plate 7 for examples of these MAC displays).

It should be noted that these MAC displays involve spectral bands from the Standard MB Combination, the Standard B/W Combination, the designed combinations, and other bands. Therefore, the spectral information does not contribute additional useful information beyond that obtained by using the Standard MB Combination. This conclusion is further supported by inspection of plates 3 through 6. It should be apparent from inspection of these plates that there are not really significant differences in tonal contrast of formation contacts in any of the bands considered.

By comparing plate 7, the MAC displays, with plates 3 through 6, it can be seen that improvement in tonal contrast has been achieved. As an example, consider the Smoky Hill Shale-Pierre Shale contact in the upper parts of the photographs on plate 7 (B and C). In comparison with plates 5 and 6 (E through H), slightly increased tonal contrast of this contact occurs on plate 7. For the same photographs and the area at the bottom, the lower Tepee Butte zone-Unit C contact of the Pierre Shale, greatly increased tonal contrast has resulted. Similar comparisons can be made for other contacts. For areas of higher relief, such as plate 7 (H and I), terrain effects are so enhanced that these MAC displays are of questionable utility.

As stated in the Introduction, tone is only one of the recognition elements used in photogeologic interpretation.

Therefore, it is concluded that, for the formations considered, there are sufficiently-detectable tonal differences in any one spectral band that these MAC displays do not aid a photo-interpreter in rock discrimination. However, if a standard photointerpretation has been completed and additional information is desired, this high-contrast, positive-negative masking technique might be useful. As an example of details that might be useful, consider plate 7 (A and D). In the center bottom of D is a blue area (shown by arrow) north of a small stream that is blue. Between these two blue areas, the mottled red area is an area of more rapid erosion and more significant development of colluvium. The mottled red area fairly accurately delimits the area of colluvium. This area cannot be interpreted to be so extensive or cannot be observed at all by tonal differences on the black and white photographs (plate 4A, plate 5E, F, G, and H). The MAC displays show this area as anomalous, and this might be useful information. Other examples can be seen by careful comparison of the plates. Therefore, when an area has been extensively studied for rock differentiation, and additional information is desired, these MAC displays may provide useful information, especially with regard to presently-active geomorphic processes and their products.

The use of more than one band with the high-contrast, positive-negative masking technique was investigated and was

not found to be significantly better than with only one band. An example is shown in the comparison of plate 7, F with G. This conclusion is in agreement with the conclusion that there is no difference between the different bands.

CONCLUSIONS

What is the value of designed multiband photography?

For rock discrimination it is not statistically possible to select a set of best bands in a practical manner from in situ rock reflectance measurements. The reason is that natural variation of formation band reflectance is large, and the differences in the contrast ratios for the bands considered are too small. Therefore, useful, information cannot be obtained from practically-obtainable, in situ reflectance measurements. Thus, multiband photography cannot be practically designed in the manner proposed.

However, equally good tonal rock discrimination can be obtained from any band. Therefore, the major significant difference in those rock reflectances observed is a relative reflectance difference that is fairly uniform throughout the photographic spectrum.

In conclusion, the designed multiband photography concept for rock discrimination, where rocks and soils are observed, is not a practical method of improving sedimentary rock discrimination capabilities for the following reasons. These reasons are (1) the difficulty of obtaining stereo pairs for interpretation, (2) the registration problem, (3) the increased problems of acquisition of multiband photography, (4) the time involved in data manipulation, and (5) the lack

of significant contrast differences between filters. Concerning the general applicability of these conclusions, the formations considered have not been selected in a statistical manner that would allow statistical inferences to be made about all rocks, or even all sedimentary rocks. However, there is no reason to suspect that the rocks and formations considered have unique reflectance properties with regard to other sedimentary rocks. Therefore, the conclusions drawn apply in detail only to the formations considered; however, generalizations of conclusions are probably valid for most sedimentary rocks.

From these conclusions come numerous implications. It is implied that there is equal information in the Standard B/W Combination and the Standard MB Combination. Both the numerical and the visual photographic analysis support this implication. Some researchers have proposed that two formations having the same or very similar Munsell color may have differences in band reflectance that can be used. Apparently, this is not significant, since the numerical data suggest that color differences are associated with band reflectance differences (see table 18 for examples of this). Therefore, from the standpoint of information content, the generalization that all bands have equal information content is valid as a first approximation.

However, when very subtle color discriminations are desired, I believe that the Standard MB Combination may provide

some additional information in comparison with all other types of photography. This implication is made only because (1) it is easier to make subtle, personally-useful color changes with the CAV if stereo pairs are not required, (2) it is easier to make MAC displays from black and white photographs than from color photographs, (3) band reflectance data do not supply a rationale for designing a Designed Combination, and (4) colors similar to true color provide a psychological interpretation advantage.

Table 18. Formation colors. See figure 8 for the band reflectances for these formations.

Formation	Munsell color
Lower Tepee	Light dusky yellow (5Y 6/2)
Rusty	Pale yellowish brown (10YR 5/3)
Smoky Hill Shale	Moderate yellowish orange (10YR 6/4)
Fountain Fm.	Dark reddish brown (10R 3/4)
Fremont Fm.	Pale red (10R 6/2)
Harding Ss.	Moderate reddish brown (10R 5/4)
Precambrian	Grayish red to pink (5R variable)

Concerning the MAC displays discussed, these techniques were found to be useful in this research for comparisons of information content between different bands. Since these comparisons were successfully made and the conclusions discussed above were derived, the MAC displays are considered a success. In addition, subtle geomorphic information was

enhanced, and the photographic color differences for many formations were significantly increased. However, new information concerning formation discrimination was not derived in this research; so the MAC techniques were not successful in this sense of "success". However, information such as geomorphic information or very subtle lithologic differentiations that are not a significant consideration in this research might be significant new information for some other problem. This statement is supported by the fact that all the MAC displays in plate 7 are not identical, and there probably are geologic reasons for the differences. Therefore, I believe that, after an interpreter has extensively studied the photography, the MAC technique is an enhancement technique that should be used if further interpretation is desired.

It was not the purpose of this research to make a comparison of multiband photography with color and color infrared photography. However, from my experience (since 1969), I have come to several conclusions concerning rock discrimination. For a general sedimentary rock mapping problem where aerial photography is not available, and considering the factors listed in table 13, the best procedure is to use color or color infrared films. This is not because there is more rock discrimination information in the color or color infrared photographs, but because the information is in a more interpretable form so rock discrimination information will be obtained in a shorter time, and color information can be useful for identification.

RECOMMENDATIONS FOR FURTHER RESEARCH

Because of the conclusions reached in this research, there are only a few recommendations for further research that are warranted. Concerning the evaluation of the multiband photography concept for rock discrimination, there are three avenues that might be followed. The first is to investigate rock reflectance properties in igneous and metamorphic environments. Two factors might allow for more success in these environments: (1) the natural variation might be significantly less, or (2) the differences in contrast ratios might be larger. From limited work in an area of altered volcanic rocks near Ophir, Colorado, it was found that the natural variation, sample variance, was as large as those observed for sedimentary rocks. Due to weather problems, the question of larger differences in contrast ratios could not be investigated.

A second avenue of investigation that might be worthwhile is to use a multichannel scanner, which is capable of narrower band widths and has higher radiometric resolution than photographic systems (Kenneth Watson, 1973, personal communication). With this approach a resolution cell could be treated as a sample, and sufficient samples could be acquired to satisfy the sample size requirements. In addition, all channels are acquired at once; therefore,

field spectral reflectance measurements are not required. Then with purely numerical data, numerous statistical techniques could be applied to select the best spectral bands, and signal-stretching and ratioing techniques could be used for enhancement. This second avenue would assume that the conclusions from the research reported here are only good as a first approximation. That is, for the radiometric accuracy of photographic systems (the first approximation) the rock reflectance differences are essentially constant relative differences; however, for a more radiometrically-accurate system, such as a multichannel scanner, there might be second-order differences that can be used advantageously.

The third avenue would approach the rock discrimination problem differently. Instead of observing soils and rocks to discriminate those rocks, the vegetation growing in and on those soils and rocks is observed. The justification for this approach is that at the Phantom Canyon Subsite the Pierre Shale had easily mappable lithologic zones that could be mapped on the ground using shrubs alone (see figure 3). Furthermore, the Paleozoic section could be readily differentiated on the basis of timber density on aerial photography. Lithologic, and possibly geochemical, information might be available through this approach.

In conclusion, three distinct approaches are proposed as warranting further research into the multiband concept of rock discrimination. These approaches are (1) applying the multiband concept to igneous and metamorphic environments, (2) using a multichannel scanner, and (3) remote sensing of vegetation for lithologic, and possibly geochemical, discrimination.

REFERENCES CITED

- Barr, D.R., 1969, Using confidence intervals to test hypotheses: *J. Quality Technology*, v. 1, p. 256-258.
- Brady, L.L., 1958, Stratigraphy and petrology of the Morrison Formation (Jurassic) in the vicinity of Canon City, Colorado: unpublished M.S. thesis, Univ. Kansas, Lawrence, Kans.
- Brainerd, A.E., Baldwin, H.L., Jr., and Keyte, I.A., 1933, Pre-Pennsylvanian stratigraphy of the Front Range in Colorado: *Am. Assoc. Petroleum Geologists Bull.*, v. 17, p. 375-396.
- Brown, T.D., 1963, Geology of the Brush Hollow area, Fremont Co., Colo.: unpublished M.S. thesis, Univ. Kansas, Lawrence, Kans.
- Colwell, R.N., (ed.), 1960, Manual of photographic interpretation: *Am. Soc. Photogram.*, Falls Church, Va., p. 857.
- Cragin, F.W., 1896, On the stratigraphy of the Platte series, or Upper Cretaceous of the plains: *Colorado Coll. Studies*, v. 6, p. 49-52.
- Cramer, J.A., Jr., 1962, The Jurassic Ralston Formation in the Southern Colorado Front Range: unpublished M.S. thesis, Univ. Kansas, Lawrence, Kans.
- Cross, Whitman, 1894, Description of the Pikes Peak, Colorado, quadrangle: *U.S. Geol. Survey Atlas*, Folio 7, 5 p.
- Egbert, D.D., and Ulaby, F.T., 1972, Effect of angles on reflectivity: *Photogram. Eng.*, v. 38, p. 556-564.
- Elias, M.K., 1931, The geology of Wallace County, Kansas: *Kansas Geol. Survey Bull.* 18, 254 p.
- Fischer, W.A., 1973, Paleoecology of the lower Harding Formation, Canon City embayment, Colorado (abs.): *Geol. Soc. America, Abs. with Programs*, v. 5, p. 480.
- Gerhard, L.C., 1961, Geology of the lower Phantom Canyon area, Fremont County, Colorado: unpublished M.S. thesis, Univ. Kansas, Lawrence, Kans.

- _____, 1964, Paleozoic paleogeology of the Canon City embayment, Colo.: unpublished Ph.D. thesis, Univ. Kansas, Lawrence, Kans.
- _____, 1967, Paleozoic geologic development of Canon City embayment, Colorado: Am. Assoc. Petroleum Geologists Bull., v. 51, p. 2260-2280.
- Gilbert, G.K., 1897, Description of the Pueblo quadrangle: U.S. Geol. Survey Geol. Atlas, Folio 36.
- Gill, J.R., Cobban, W.A., Scott, G.R., and Burkholder, R.E., 1972, Section of Pierre Shale measured in the Florence and Canon City Quadrangles, Colorado: U.S. Geol. Survey open file report, 6 p.
- Hubert, J.F., 1960, Petrology of the Fountain and Lyons Formations, Front Range, Colorado: Colo. Sch. Mines Quart., v. 55, 242 p.
- Jones, D.A., and Karson, M.J., 1972, On the use of confidence regions to test hypotheses: J. Quality Technology, v. 4, p. 156-158.
- Koch, G.S., Jr., and Link, R.F., 1920, Statistical analysis of geological data: John Wiley and Sons, Inc., New York, v. 1, 375 p.
- Lavington, C.S., 1933, Montana group in eastern Colorado: Am. Assoc. Petroleum Geologists Bull., v. 17, p. 397-410.
- Lucken, J.E., 1964, Tectonics of southern Phantom Canyon, Fremont Co., Colo.: unpublished M.S. thesis, Univ. Kansas, Lawrence, Kans.
- Maher, J.C., 1953, Paleozoic history of southeastern Colorado: Am. Assoc. Petroleum Geologists Bull., v. 37, p. 2475-2489.
- Mann, C.J., 1957, Geology of the Chandler Syncline, Fremont County, Colorado: unpublished M.S. thesis, Univ. Kansas, Lawrence, Kans.
- Meek, F.B., and Hayden, F.V., 1862, Description of new Lower Silurian (Primordial), Jurassic, Cretaceous, and Tertiary fossils, collected in Nebraska Territory, with some remarks on the rocks from which they were obtained: Acad. Nat. Sci. Philadelphia Proc., 1861, p. 415-447.
- Monk, W.J., 1954, A faunal study of the Fremont Formation in the Canon City embayment, Colorado: unpublished M.S. thesis, Univ. Oklahoma, Norman, Okla.

- Mudge, B.F., 1877, Notes on the Tertiary and Cretaceous periods of Kansas: U.S. Geol. Geog. Survey Terr. (Hayden) 9th Ann. Rept., p. 277-294.
- Ogden, Lawrence, 1958, Permian-Jurassic facies, Colorado Front Range and adjacent areas: unpublished D.Sc. thesis, Colorado School of Mines, Golden, Colo.
- Ray, R.G., 1960, Aerial photographs in geologic interpretation and mapping: U.S. Geol. Survey Prof. Paper 373, 230 p.
- Robertson, B.G., 1957, Stratigraphy of the Williams Canyon Formation: unpublished M.S. thesis, Univ. Oklahoma, Norman, Okla.
- Ross, D.S., 1973, Simple multispectral photography and additive color viewing: Photogram. Eng., v. 39, p. 583-591
- Rowan, L.C., Billingsley, F.C., Gillespie, H.R., Goetz, A.F.H., Wetlaufer, P.H., 1973, Discrimination of limonitic zones and of rock types using ERTS imagery: Geol. Soc. America Abs. with Programs, v. 5, p. 787.
- Sackett, D.H., 1961, Geology of the Garden Park area, Fremont Co., Colo.: unpublished M.S. thesis, Univ. Kansas, Lawrence, Kans.
- Saylor, W.W., 1955, Late Paleozoic and Early Mesozoic stratigraphy of eastern Canyon City embayment, Colorado: unpublished M.S. thesis, Univ. Oklahoma, Norman, Okla.
- Scott, G.R., 1963a, Quaternary geology and geomorphic history of the Kassler Quadrangle, Colorado: U.S. Geol. Survey Prof. Paper 421-A, 70 p.
- _____, 1963b, Bedrock geology of the Kassler Quadrangle, Colorado: U.S. Geol. Survey Prof. Paper 421-B, 125 p.
- _____, 1969, General Engineering Geology of the northern part of Pueblo, Colo.: U.S. Geol. Survey Bull. 1262, 131 p.
- Scott, G.R., and Cobban, W.A., 1964, Stratigraphy of the Niobrara Formation at Pueblo, Colorado: U.S. Geol. Survey Prof. Paper 454-L, 30 p.
- Smith, J.T., Jr., and Anson, Abraham, 1968, Manual of color aerial photography: Falls Church, Va., 550 p.

- Sweet, W.C., 1954, Harding and Fremont Formations, Colorado: Am. Assoc. Petroleum Geologists Bull., v. 38, p. 284-305.
- Tolgay, M.Y., 1952, A sedimentary study of the Harding Formation near Canon City, Colorado: unpublished M. Geol. Eng. thesis, Univ. Oklahoma, Norman, Okla.
- Vincent, R.K., 1972, An ERTS multispectral scanner experiment for mapping iron compounds in Proceedings of the eighth international symposium remote sensing of environment: Willow Run Laboratories, Ann Arbor, Mich., p. 1235-1243.
- Walcott, C.D., 1892, Preliminary notes on the discovery of a vertebrate fauna in Silurian (Ordovician) strata: Geol. Soc. America Bull., v. 3, p. 153-172.
- Webster, G.D., 1959, Geology of the Canon City-Twin Mountain area, Fremont County, Colo.: unpublished M.S. thesis, Univ. Kansas, Lawrence, Kans.
- Warren, T.H., 1960, Stratigraphy and sedimentation of the Pennsylvanian-Permian Fountain Formation, Fremont County, Colorado: unpublished M.S. thesis, Univ. Oklahoma, Norman, Okla.
- Williston, S.W., 1893, The Niobrara Cretaceous of western Kansas: Kansas Acad. Sci. Trans., v. 13, p. 107-111.
- Yost, E.F., and Wenderoth, Sondra, 1967, Multispectral color aerial photography: Photogram. Eng. v. 33, p. 1020-1033.

APPENDIX A: REDAT AND REFLCT COMPUTER PROGRAMS

Two computer programs, REDAT and REFLCT, were written to facilitate the reduction of the FWP band reflectance data. The first program, REDAT, was written by Mr. Art Kuczek for teletype interfacement with the Colorado School of Mines PDP-10. REDAT takes the meter readings from the FWP and calculates band reflectance using the calibration standards data. Figure A1 is the input data format. The calculation procedure is explained in figure 6 (p.27). REDAT produces two copies of the calculated band reflectance, one for a permanent record and one for input into REFLCT. This second copy is then manually reformatted as in figure A2 and then entered into REFLCT.

FWP Data Sheet 1

Formation _____

Formation _____

Location _____

Comments _____

Date data collected: _____ Time: Start Stop

Filter # Source Meter Readings

Obsv. of Data

NF S3.5N 8.7

NF S18% 17.4

NF S7.5N 50.0

NF T

2C S3.5N 8.6

2C S18% 15.7

2C S7.5N 50.4

2C T

Figure A1. Input data sheet for REDAT. This is only part of the form; it continues in a similar manner to include the rest of the filters. Filter order is based on ease of measurement.

FORMATION _____

Plot desired _____ Colored Plot _____

Standard Run _____ Semi-Standard Run _____ Non-Standard _____

Formation _____

Location _____

Comments _____

% Confidence _____

Will all filters have same # of observations? _____

 If YES, # observations _____

T-value _____

Correction Factor for variance of median _____

Filter	# Observ.	Band Reflectance	t-value
47B			
57			

Figure A2. Input data Sheet for REFLCT. This is only part of the form; it continues in a similar manner to include the rest of the filters. Filter order is based on pass band.

REFLCT was written by Mr. Greg L. Kaup for teletype interfacement with the Colorado School of Mines PDP-10. REFLCT uses standard formulas to calculate the means, medians, variances, standard deviations, and confidence intervals. The confidence interval on the median can be corrected for the fact that the median is a poorer estimator of the population mean by entering an appropriate correction factor. However, in this research, the median was used

only when the sample was very skewed, and then a correction factor of 1.0 was used for the confidence interval on the median. There are two outputs from REFLCT, a printout for each filter of the input with calculated statistics and a log band reflectance plot of means, medians, confidence intervals, and observations for all filters for each formation. Figure A3 is one page of the printout. There are thirteen pages in an actual printout, one for each filter. Figure A4 is the log reflectance plot for one formation.

The flow of these two programs is diagrammed in Figure A5. Both programs are available through the Geology Department, Colorado School of Mines, Golden, Colorado 80401.

Pierre Shale, Lower Tepee Zone
Phantom Canyon Rd

For Filter 87C ---

Percent of Confidence: -----	80
T-value: -----	1.42
Correction Factor for Variance of the Median: -----	1.00
Number of Observations: -----	8

Data Points:

21.000	22.000	23.000	25.000	27.000
28.000	28.000	34.000		

Sum of the Observations: -----	208.00000
Sum of the Square of the Observations: -----	5532.00000

Mean: -----	26.00000
Variance of the Mean: -----	17.71429
Standard Deviation of the Mean: -----	4.20883
Coefficient of the Variation of the Mean: --	0.16188

The 80% Confidence Interval about the Mean
with 8 Observations is 2.3894E+01 to 2.8106E+01

Median: -----	26.00000
Variance of the Median: -----	17.71429
Standard Deviation of the Median: -----	4.20883
Coefficient of the Variation of the Median: -	0.16188

The 80% Confidence Interval about the Median
with 8 Observations is 2.3894E+01 to 2.8106E+01

Figure A3. Example of computer printout that is generated for each filter for each formation.

SMOKY HILL SHALE
PHANTOM CANYON
95% CONFIDENCE

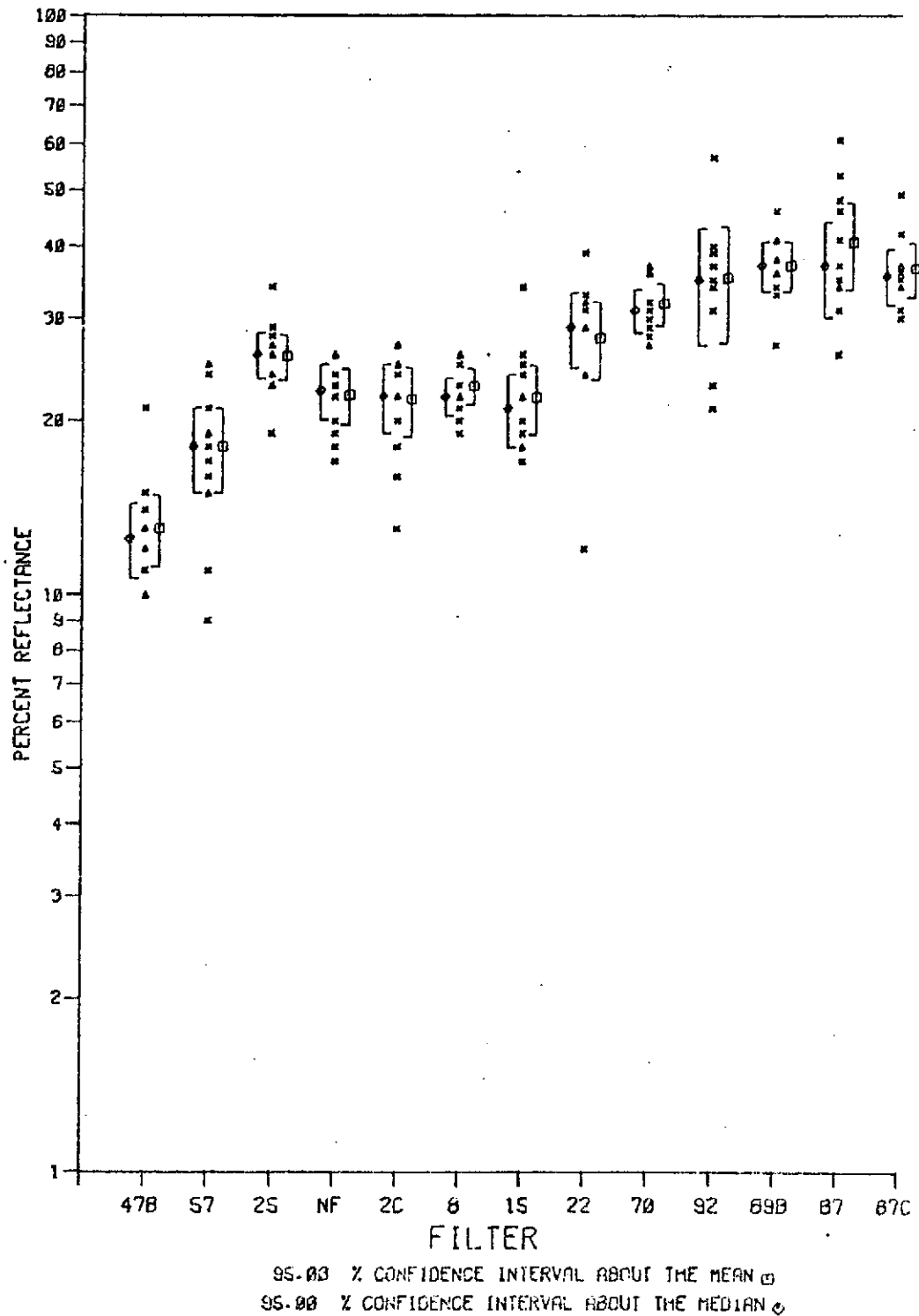


Figure A4. Computer-generated log reflectance plot. The x's are single data points, and the triangles are multiple data points. The brackets are confidence intervals.

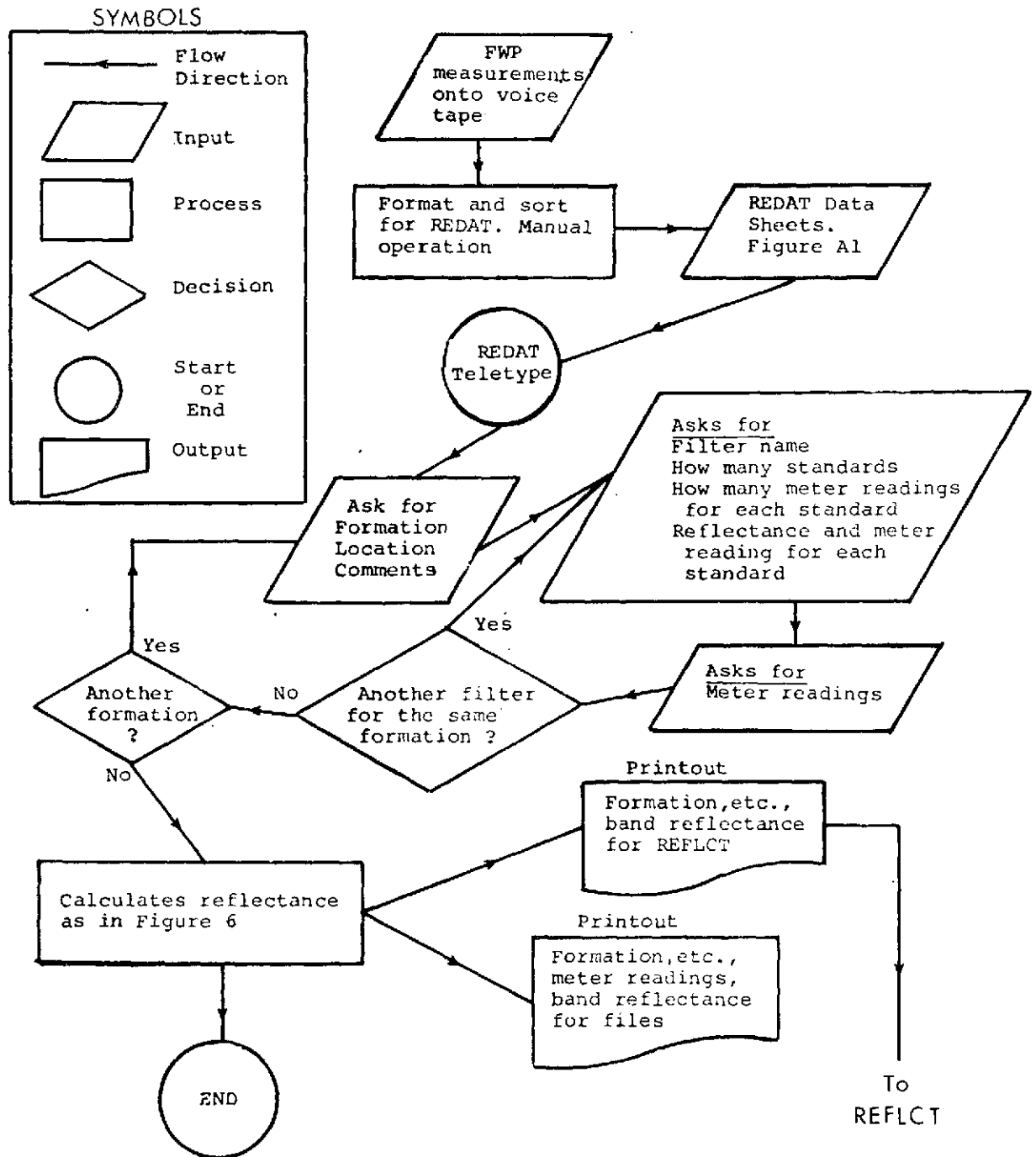
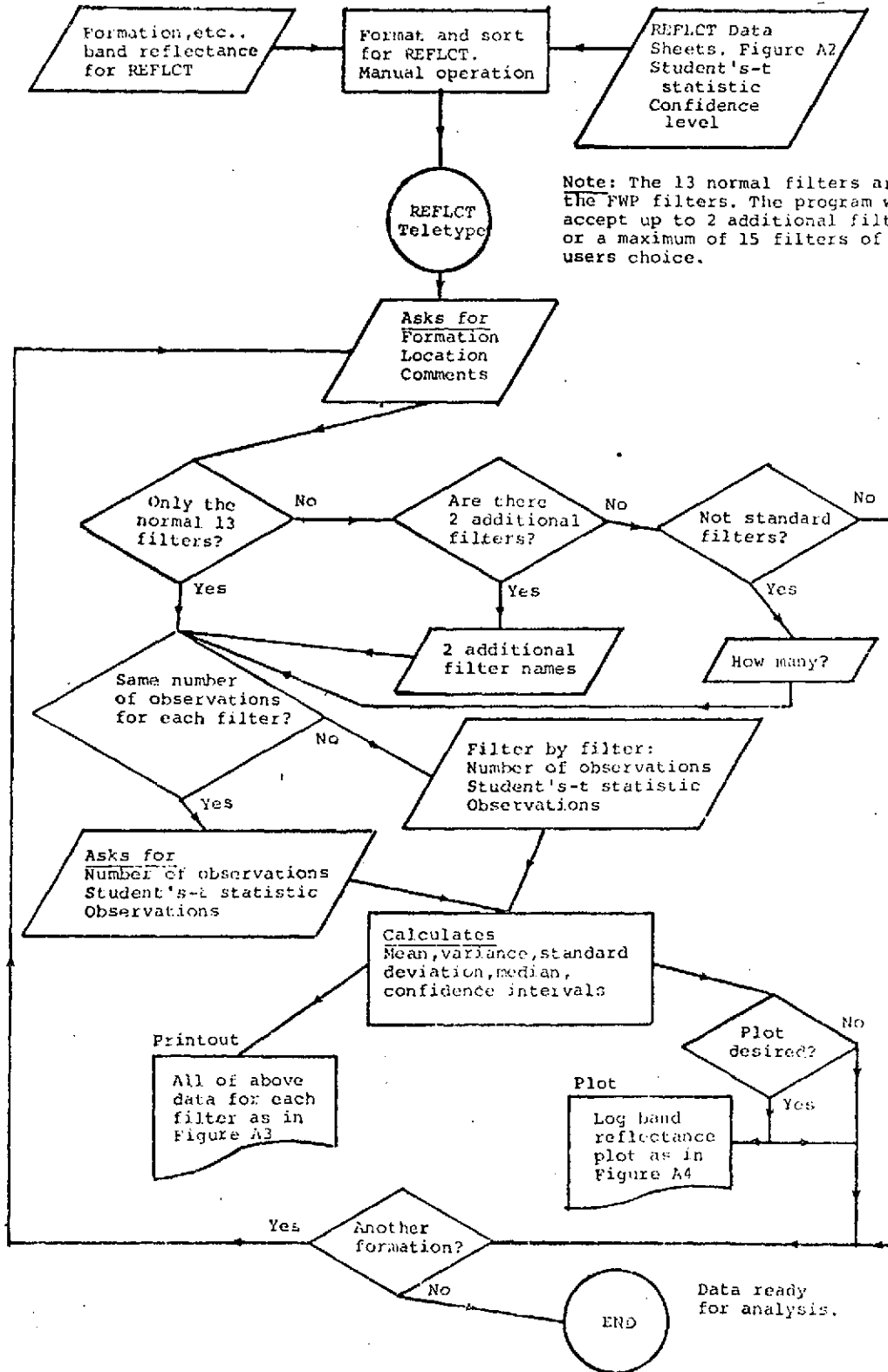


Figure A5. FWP data reduction flow chart. REDAT is on the first page and REFLCT is on the second page.



Note: The 13 normal filters are the FWP filters. The program will accept up to 2 additional filters or a maximum of 15 filters of the users choice.

Figure A5. (continued)

APPENDIX B: DARKROOM PROCEDURES FOR THE HIGH-CONTRAST
POSITIVE-NEGATIVE MAC DISPLAYS

Ratioing and signal-stretching techniques are being suggested by several investigators as useful techniques for the geologic analysis of ERTS data and other numerical types of remote sensing data (Vincent, 1972; Rowan and others, 1973). However, these techniques require considerable computer power, expertise, and expense. Less expensive and simpler techniques that I have used are the photographic equivalents of ratioing and signal-stretching: positive-negative masking and high-contrast copying, respectively.

The basic concept is that film density differences that cannot be discriminated by the human eye on the original are amplified by the use of high-contrast copies made at different exposures. Then by the use of positive and negative high-contrast copies and a method of color-coding these various copies, such as a color additive viewer, a diazo process, or a photographic color printing technique, the images can be recombined. These techniques can be used advantageously with a single photograph, multiband photography, ERTS data, or any other type of photographic data. These techniques are known to photographers as posterization techniques.

A significant limitation of these techniques arises with large-scale photography in areas of high relief. In

such situations, shadows are generally greatly enhanced, and the resulting changes in the scene's appearance in the high-contrast, positive-negative mask make recognition of familiar things very difficult. Thus, on large-scale photography the technique seems to work best for areas of uniform slopes and slight relief. On small-scale photography this probably is not a significant problem.

Procedure

The supplies needed to use this technique are listed in table B1. For a semi-quantitative procedure, the additional supplies listed are also needed. A darkroom outfitted for black and white printing is necessary.

Table B1. Supplies needed to make high-contrast, positive-negative masks.

Essential Supplies

1. High-Contrast film, Kodalith or DuPont Cronar S Litho.
2. Kodalith Developer.
3. Standard stop bath, fixer, and hypo clearing agent.
4. Large format contact printer or piece of plate glass.

Additional Supplies

1. Density Wedge, available from Kodak, does not need to be accurately calibrated.

The basic procedure is to make contact prints of the original photograph onto high-contrast film. The exposure should be that producing a middle-gray on the high-contrast film from the density level at which the information to be enhanced occurs. Then other exposures above and below this

exposure will isolate the desired density. An exposure change of one f-stop will change this middle-gray producing density by 0.3 density units, a $\frac{1}{2}$ f-stop change will change this density 0.15 units, and so on. To isolate the desired density, the exposures above and below this density can be combined in positive-negative mask and color coded.

When anomalous features are seen on the individual high-contrast positive and negative copies, these positives and negatives can be registered manually and/or optically in the CAV and color coded. The objective of the color coding is to isolate unique information in the display and to enhance areas with information from several masks. This explanation is, of necessity, rather general, since each photograph worked with is a unique situation and the results cannot be predicted well. However, many different combinations of masks can be made rapidly and cheaply, so the trial and error method is best until some experience is gained. One useful idea is to select copies that obviously isolate known features so that these features do not distract the interpreter.

To calibrate the procedure, a density wedge can be used as the original. Then the effects of specific exposures and exposure changes with the equipment being used can be calibrated. This will not be an exact calibration; however, it will allow semi-quantitative correlation with signal levels and might prove to be useful when working with other

photography. In addition, the experience gained from working with the density wedge greatly aids understanding of the results.

APPENDIX C: EXPLANATION OF PHOTOGRAPHIC PLATES

In all plates north is to the top.

PLATE 3: Standard Multiband Combination. Scenes A, B, and C are color, color infrared and color infrared displays, respectively. Scenes A and B are in secs. 20, 21, 28, and 29, T. 18 S., R. 69 W., of the Phantom Canyon Subsite. Scene C is in secs. 4, 5, 8, and 9, T. 18 S., R. 69 W., of the Phantom Canyon Subsite. Scenes D, E, and F all are Standard MB Combination (47B coded blue and 88A coded red). Scene D is in secs. 28 and 29, T. 18 S., R. 69 W., of the Phantom Canyon Subsite. Scene E is in secs. 35 and 36, T. 19 S., R. 69 W., of the Florence SE Subsite. Scene F is in sec. 13, T. 18 S., R. 71 W., and sec. 18, T. 18 S., R. 70 W., of the Gorge Hills Subsite. See plate 1 for the geology.

PLATE 4: Standard Black and White Combination and Contrast Ratio Test Combination. Scenes A and B were taken with panchromatic film and a Wratten 12 and are examples of the Standard B/W Combination. Scene A is in secs. 20, 21, 22, 27, 28, and 29, T. 18 S., R. 69 W. Scene B is in secs. 4, 5, 8, and 9, T. 18 S., R. 69 W. Both A and B are in the Phantom Canyon Subsite. See plate 1 for the geology. Scenes C, D, E, and F are the Contrast Ratio Test Combination and the filters are Wratten 8, 15, 70, and 92, respectively. Filters 8 and 15 were predicted

to be better than filters 70 and 92. Scenes C, D, E, and F are in secs. 13, 14, 23, and 24, T. 7 S., R. 69 W., in the Kassler quadrangle.

PLATE 5: Phantom Canyon Designed Combination. Scenes A and E, B and F, C and G, D and H are Wratten 57, 22, 90, and 70, respectively. Scenes A, B, C, and D, of the Paleozoic section, are in secs. 4, 5, 8, and 9, T. 18 S., R. 69 W., of the Phantom Canyon Subsite. Scenes E, F, G, and H, of the Cretaceous shale section, are in secs. 20, 21, 28 and 29, T. 18 S., R. 69 W., of the Phantom Canyon Subsite. See plate 1 for the geology. The major significance of these scenes is that tonal discriminations are all essentially the same.

PLATE 6: Gorge Hills - Florence SE Designed Combination. This plate is the same as plate 5 except the filters are Wratten 47 B, 8, 25, and 87. See plate 1 for the geology. Again, the significant point is that tonal discriminations in all the bands are essentially the same on this plate and in comparison with plate 5.

PLATE 7: MAC Displays. Scenes A through I were made using the high-contrast, positive-negative masking technique (see Appendix B) using the scenes from the Wratten 12, 47B, 57, 88A, 70, 25, 25 and 88A, 47B, and 87, respectively. Scenes A, B, C, D, and E are in secs. 20, 21, 28, and 29,

T. 18 S., R. 69 W., of the Phantom Canyon Subsite. Scenes F and G are in secs. 25, 26, 35, and 36, T. 19 S., R. 69 W., of the Florence SE Subsite. Scene H is in secs. 13 and 24, T. 18 S., R. 71 W., and secs. 18 and 19, T. 18 S., R. 70 W., of the Gorge Hills Subsite. Scene I is in secs. 4, 5, 8, and 9, T. 18 S., R. 69 W., of the Phantom Canyon Subsite. See plate 1 for the geology. The significant points of these plates are (1) MAC displays of equal quality can be made with any spectral band, (2) MAC displays are not significantly better than the black and white photographs for general geologic mapping, and (3) in rugged terrain (scenes G and I) information loss is very significant. Direct comparisons can be made between plate 7 (A through E) and plates 3 (A, B, and D), 4 (A), and 5 and 6 (E through H); between plate 7 (F through G) and plate 3(E); between plate 7 (H) and plate 3 (F); and between plate 7 (I) and plates 3 (C), 4(B), and 5 and 6 (A through D).

Generalized geologic maps for plates 3 through 7.

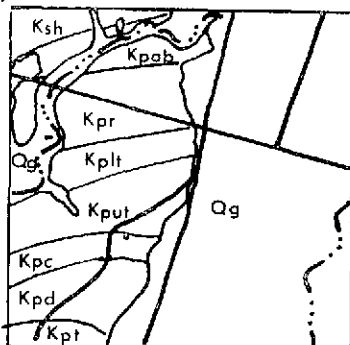
Symbols

— Road - - - - - Stream ——— Contact

All formation symbols are as on plate 1.

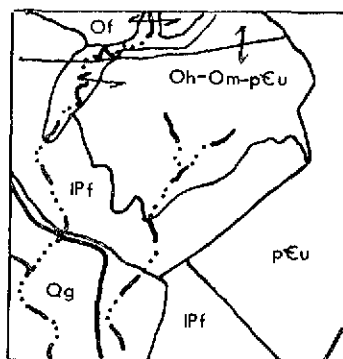
In all cases north is to the top. The scale is variable due to the photography being acquired on several different flights; however, the scale is approximately 1:55,000.

GENERALIZED MAPS

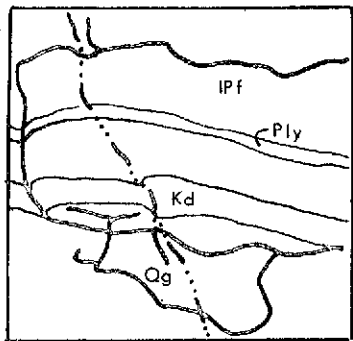


PLATE

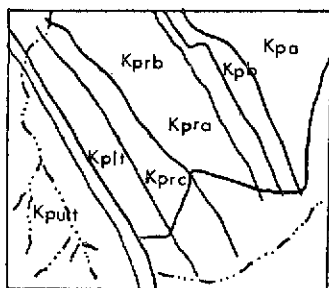
3 A, B, and D
4 A
5 E, F, G, and H
6 E, F, G, and H
7 A, B, C, D, and E



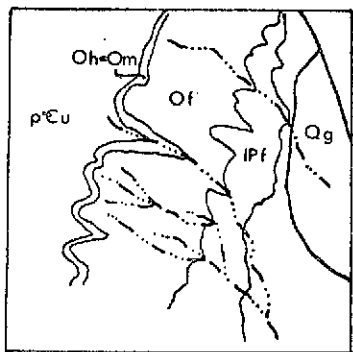
3 C
4 B
5 A, B, C, and D
6 A, B, C, and D
7 I



4 C, D, E, and F



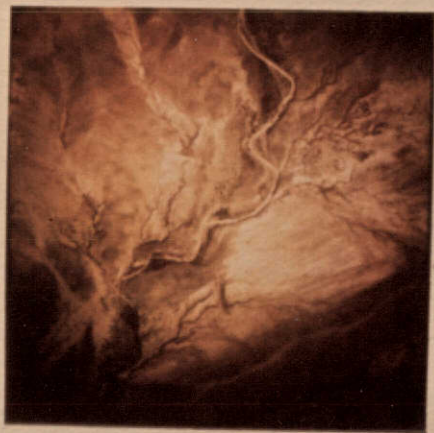
3 E
7 F and G



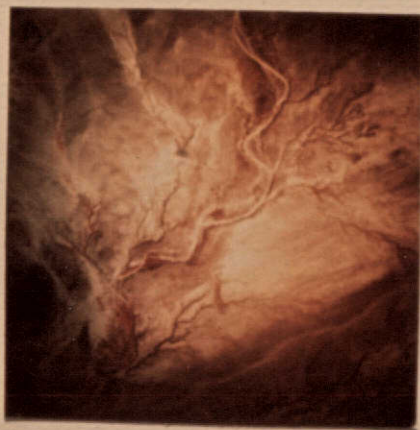
3 F
7 H (southern half of the map)

LOCATIONS AND GENERALIZED GEOLOGIC MAPS FOR PLATES
3 THROUGH 7 ARE IN APPENDIX C.

STANDARD COMBINATION



A Color Display



B CIR Display



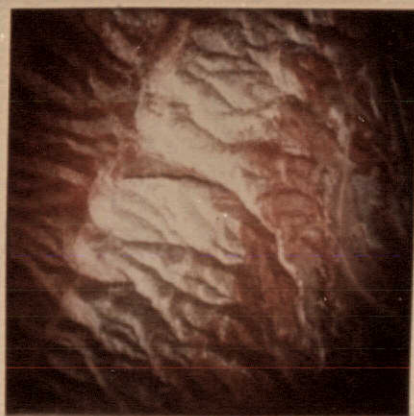
C CIR Display



D Nonstandard Coding



E Nonstandard Coding



F Nonstandard Coding

STANDARD BLACK AND WHITE COMBINATION

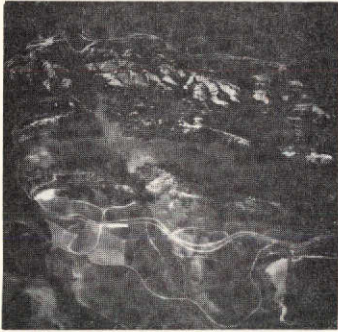


A Wratten 12

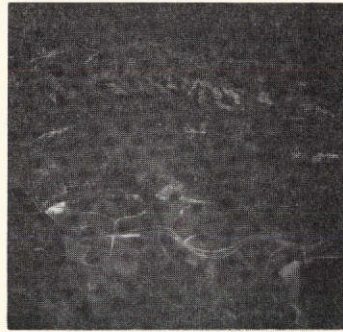


B Wratten 12

CONTRAST RATIO TEST COMBINATION



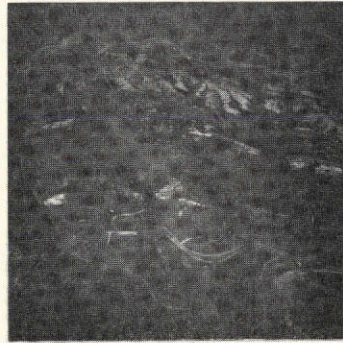
C Wratten 8



D Wratten 15



E Wratten 92



F Wratten 70

PHANTOM CANYON DESIGNED COMBINATION



A Wratten 57



B Wratten 22



C Wratten 92



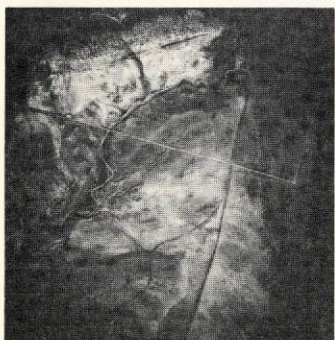
D Wratten 70



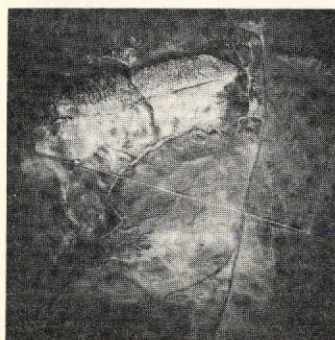
E Wratten 57



F Wratten 22



G Wratten 92



H Wratten 70

GORGE HILLS-FLORENCE SE DESIGNED COMBINATION



A Wratten 47B



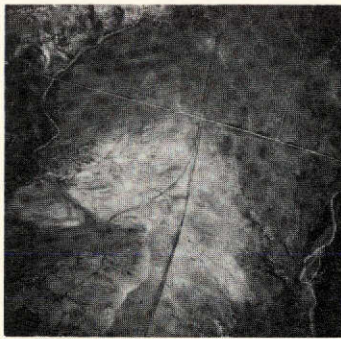
B Wratten 8



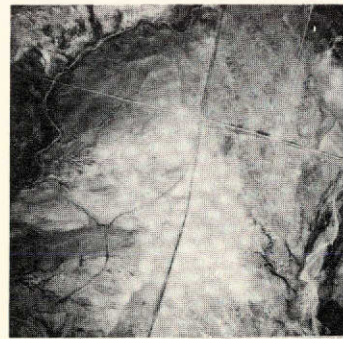
C Wratten 25



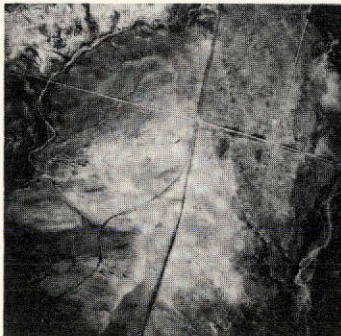
D Wratten, 87



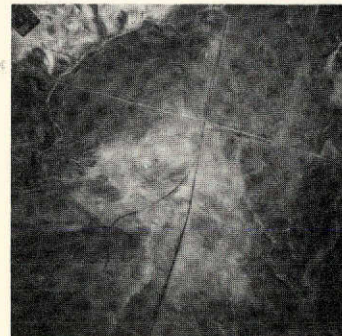
E Wratten 47B



F Wratten 8

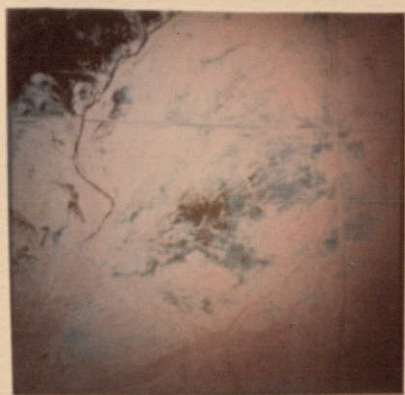


G Wratten 25

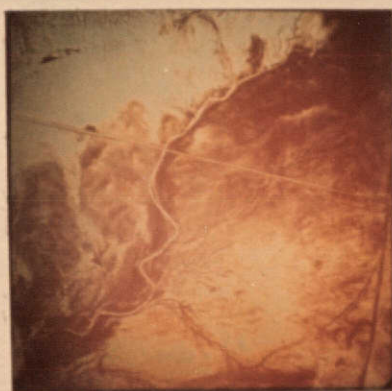


H Wratten 87

MAC DISPLAYS



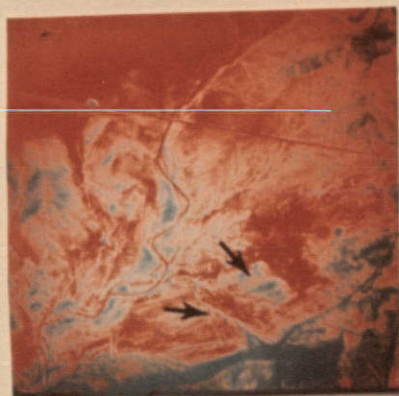
A Wratten 12



B Wratten 47B



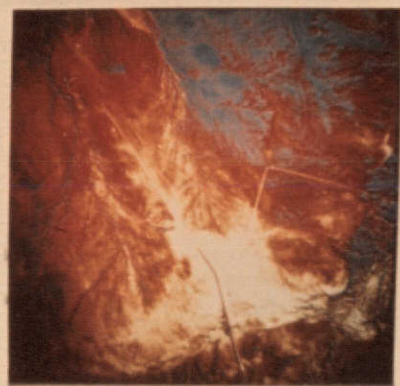
C Wratten 57



D Wratten 88A



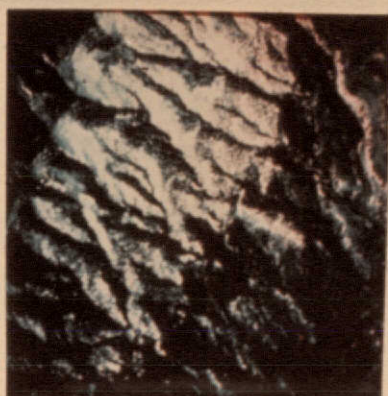
E Wratten 70



F Wratten 25



G Wrattens 25
and 88A



H Wratten 47B



I Wratten 87